STRATIGRAPHIC INVESTIGATION OF THE NORTH WESTSIDE BASIN OF SAN FRANCISCO AND NORTHERN SAN MATEO COUNTY

A thesis submitted to the faculty of
San Francisco State University
in partial fulfillment of
the requirements for
the degree

Master of Science
in
Applied Geosciences

by

Terence McGuire

San Francisco, California

May, 2009

CERTIFICATION OF APPROVAL

I certify that I have read "Stratigraphic investigation of the North Westside Basin of San Francisco and northern San Mateo County," by Terence McGuire, and that in my opinion this work meets the criteria for approving a thesis submitted in partial fulfillment of the requirements for the degree: Master of Science in Applied Geosciences at San Francisco State University.

_____

Dr. Karen Grove
Professor of Geosciences

_____

Dr. John Caskey
Professor of Geosciences

_____

Dr. Andrea Fildani
Geologist Chevron Technology Corporation

STRATIGRAPHIC INVESTIGATION OF THE NORTH WESTSIDE BASIN OF SAN FRANCISCO AND NORTHERN SAN MATEO COUNTY

Terence McGuire
San Francisco State University
2009

The Merced and Colma Formations are the primary lithologic units in the North Westside Groundwater Basin. These marginal marine units are exposed in the sea cliffs between San Francisco and Daly City, and are packaged in unconformity-bounded sequences that were deposited during Pleistocene sea-level changes within a subsiding basin associated with the San Andreas fault system. This study examines formation sequences S–Y, and uses well data to correlate coastal exposures to inland units and produce a subsurface-stratigraphic model. The model indicates that most upper Merced sequences were deposited in a beach-barrier-embayment environment. High-energy, nearshore facies exposed along the coast transition inland to low-energy, fine-grained, paleoembayment sediments that now form a series of aquitards dividing the subsurface strata into three aquifers. The strata form a northwest–southeast trending, asymmetric anticline–syncline pair adjacent to the Serra blind thrust fault. An analysis of Merced and Colma age data and the Pleistocene sea-level curve indicates that transgressions associated with sequences F-O may have been tectonically driven, whereas transgressions from sequence P upwards may have been eustatically driven.

I certify that the abstract is a correct representation of the context of this thesis.

_____ _____

Chair, Thesis Committee Date

ACKNOWLEDGEMENTS

My deepest thanks to my advisor Dr. Karen Grove, with whom I spent many hours discussing well cuttings, well logs and the Merced Formation. Thank you also to my committee members John Caskey and Andrea Fildani for their insights and advice throughout this process. I am very grateful to Greg Bartow and Jeff Gilman of the San Francisco Public Utilities Commission for providing guidance, data and partial funding of this project. I'd also like to thank Tom Elson and Luhdorff and Scalmanini Consulting Engineers for providing much of the well data. Both Drew Kennedy and Erdmann Rogge were very generous in providing additional data which was critical to this study. Finally, many thanks to my co-workers at Harris' Steakhouse who have been like a second family, my wife Liz for her patience and support and to my son Jack, who makes all this work worthwhile every time we play in fine to medium, well-rounded, very well-sorted sand.

TABLE OF CONTENTS

LIST OF TABLES

Table

LIST OF FIGURES

Figure

LIST OF PLATES

LIST OF APPENDICES

Appendix

INTRODUCTION

The Plio-Pleistocene Merced Formation, exposed in the coastal bluffs between San Francisco and Daly City, extends inland to the southeast where it controls most of the groundwater flow in the Westside Groundwater Basin (Figure 1; Rogge, 2003). The northeast-dipping section is composed of over 1700 m of poorly consolidated sand, mud and rare gravel generally packaged into dozens of upward-shallowing, unconformity-bounded sequences (Clifton et al., 1988). Hall (1965) more broadly divided the Merced into upper and lower units. The lower unit is composed of mostly fine-grained shelf deposits, whereas the upper Merced is composed of predominantly coarser-grained nearshore and backshore sediments. In this study I focus on the upper Merced Formation in the North Westside Basin (Figure 1); specifically, I examine sequences S-Y of Hunter et al. (1984)(Figure 2; Plate 1) that mantle the bedrock surface below Lake Merced and are the primary aquifer forming strata in this area. I also include the late Pleistocene Colma Formation (sequence Z), which overlies the Merced and forms the upper part of the aquifer system.

The North Westside Groundwater Basin is a vital groundwater resource used by the City of San Francisco and by San Mateo County. It is used for both drinking water and irrigation. The San Francisco Public Utilities Commission (SFPUC) and consultants working for the City are currently monitoring groundwater quality, monitoring changes

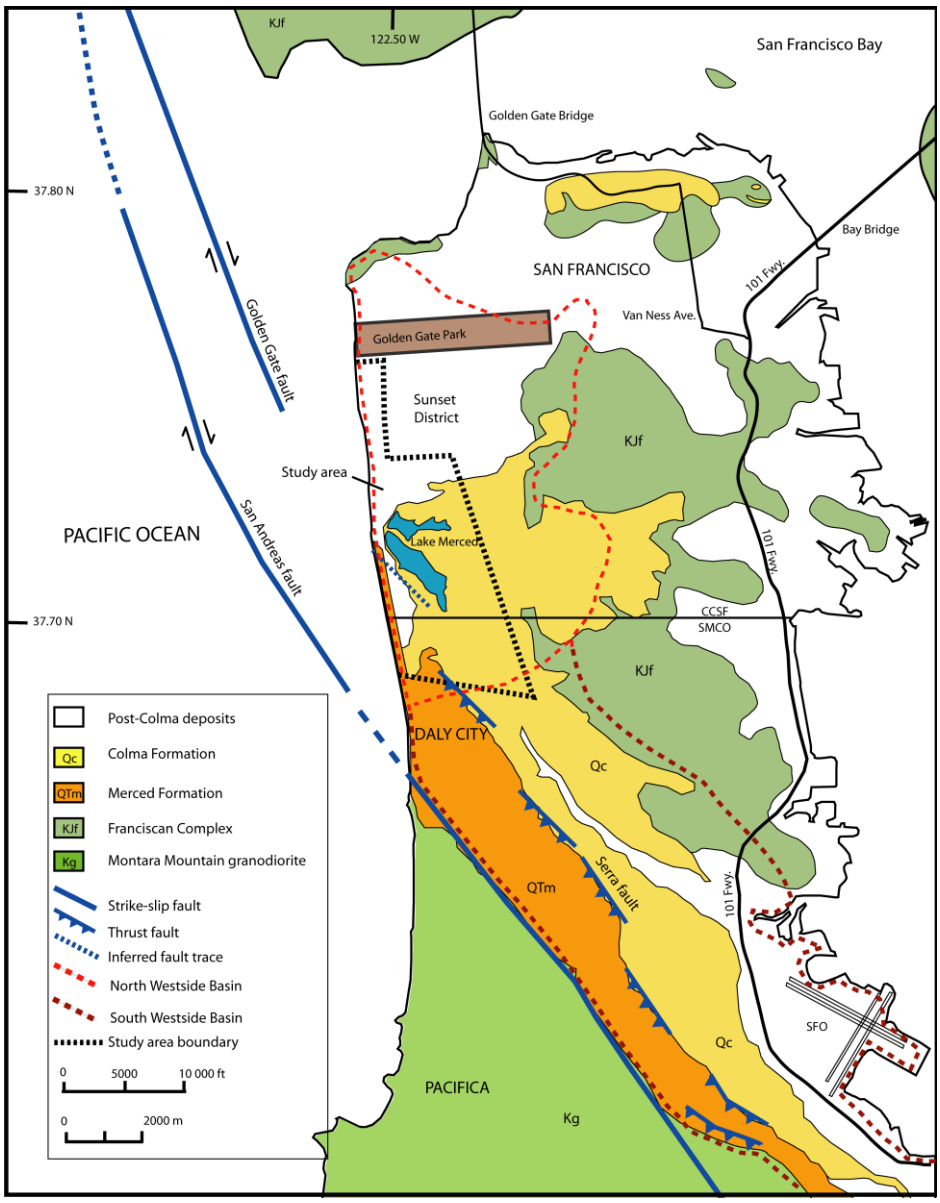

Figure 1. Location map showing regional geology, study area and North and South Westside Basin boundaries. Map adapted from Clifton and Hunter (1987). Geology adapted from Bonilla (1971) and offshore fault traces after Bruns et al. (2002).

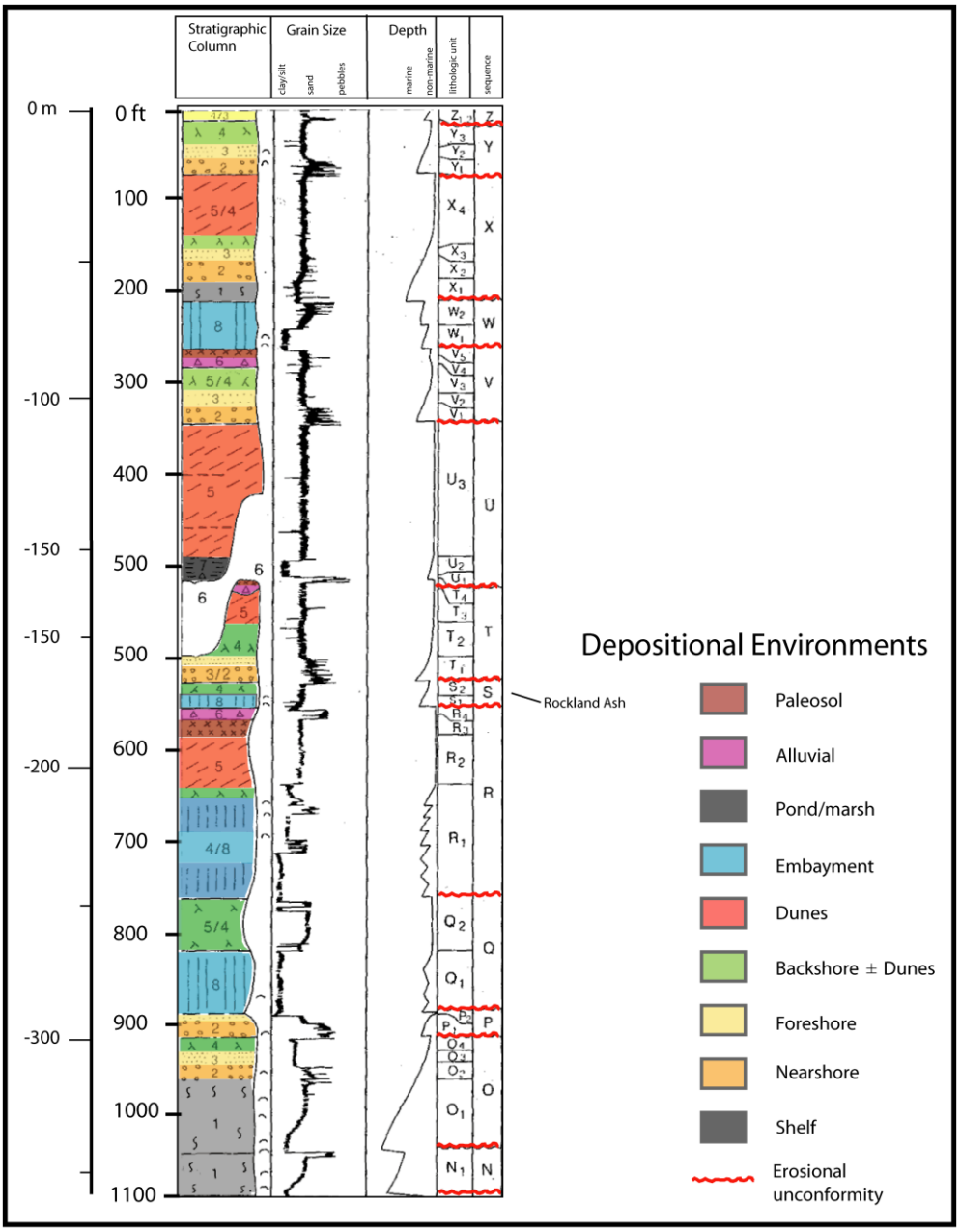

Figure 2. Clifton et al.'s (1988) coastal stratigraphic column of the upper Merced Formation sequences focused on in this study.

in the groundwater system due to the addition of new production wells, and developing a pilot conjunctive use program in which water will be stored during wet years and drawn upon in emergency situations (Nzewi, 2006). Most recently, Luhdorff and

Scalmanini Consulting Engineers reported on the basin's water quality, hydrogeology and stratigraphy in two reports (LSCE, 2004 and 2006).

The goal of my thesis research was to build upon and refine previous hydrostratigraphic studies, providing a more thorough analysis of the sediments, their environments of deposition, and the geometry of aquifer units. I compiled and analyzed the existing stratigraphic data and used them to create a new model of sedimentary facies and their connections to surface outcrops. This updated subsurface model will enable the SFPUC to better manage this valuable resource and the results also further our understanding of the tectono-stratigraphic evolution of the Merced and Colma Formations.

In this study I included six cross sections (Plates A-F) that depict the marginal-marine sedimentary units in the Lake Merced area (Figure 3). Sections A-A' and D-D' are coast parallel, B-B' and C-C' are coast-oblique, and E-E' and F-F' are roughly coast-perpendicular and serve as tie lines. In building the cross sections I used geophysical and lithologic logs, outcrop data, surface mapping and well cuttings to produce the updated subsurface model. Based on the resultant stratigraphic model, it appears that sequences S through Z were deposited in a beach/barrier/embayment environment (Figure 4) with a paleo-coastline that trended more northwesterly than the present shoreline.

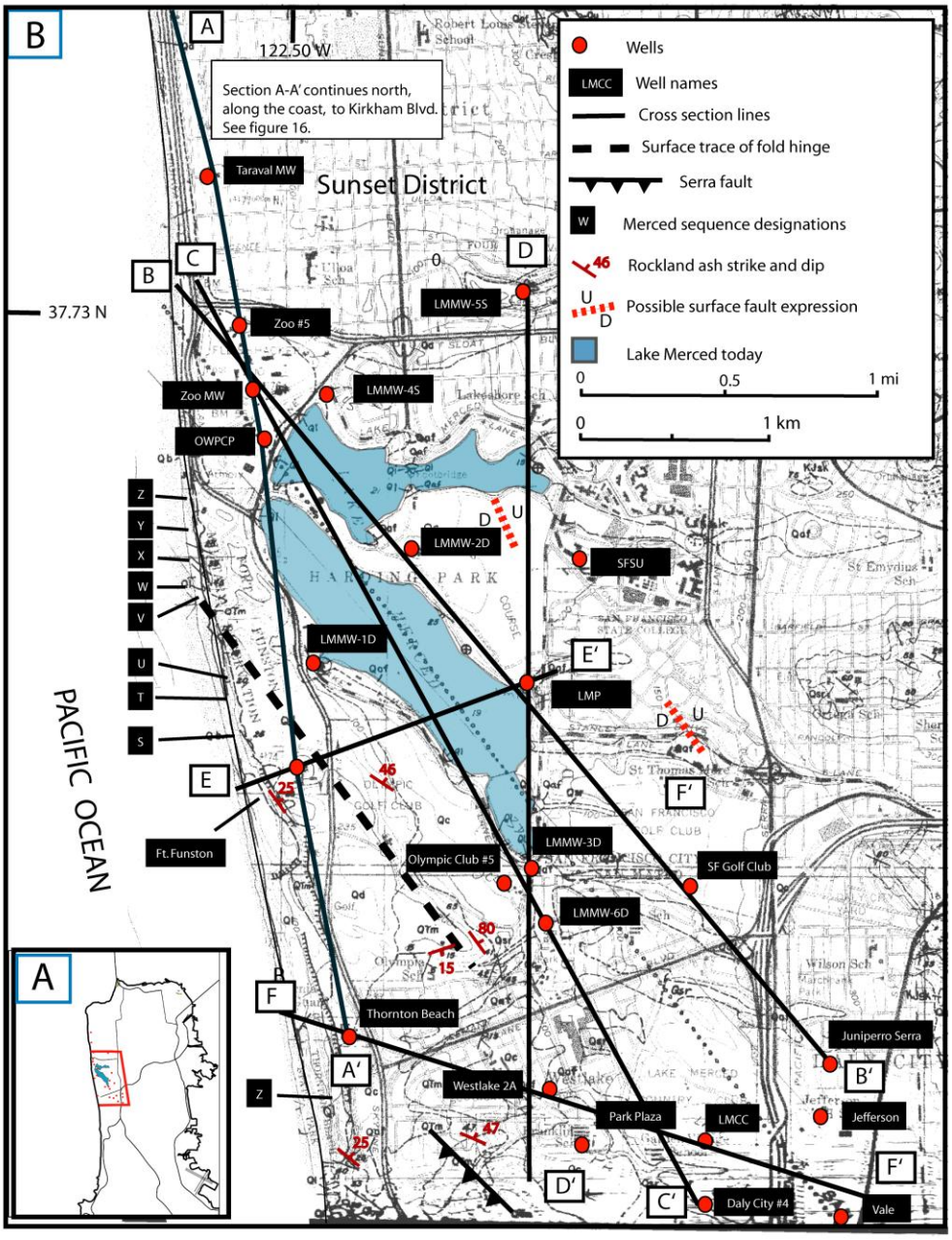

Figure 3. Location map. "B" is expansion of inset map "A". Map shows wells used in the study, cross section lines and the locations of Merced Formation sequences in coastal outcrop as defined by Clifton et al. (1988). Base map from Bonilla (1971).

The fine-grained sediments associated with these embayments appear to now form a series of vertically separated aquitards that divide the strata beneath Lake Merced into three compartmentalized aquifers that have been folded and form a broad northwest–southeast trending, asymmetric syncline with fold limbs that become more open and flat to the northwest (Figure 5; Plates A-F).

In the following sections I describe the Merced and Colma Formations; their geologic setting; my methods and initial correlation strategy; the structure of the Merced basin; the sedimentology and stratigraphy of units that form the relevant aquifer-forming strata; a general paleo-geographic model; the location of primary aquitards and aquifers and a comparison of water quality data to stratigraphic data. Finally, I discuss Pleistocene sea level fluctuations as related to upper sequences of the Merced Formation.

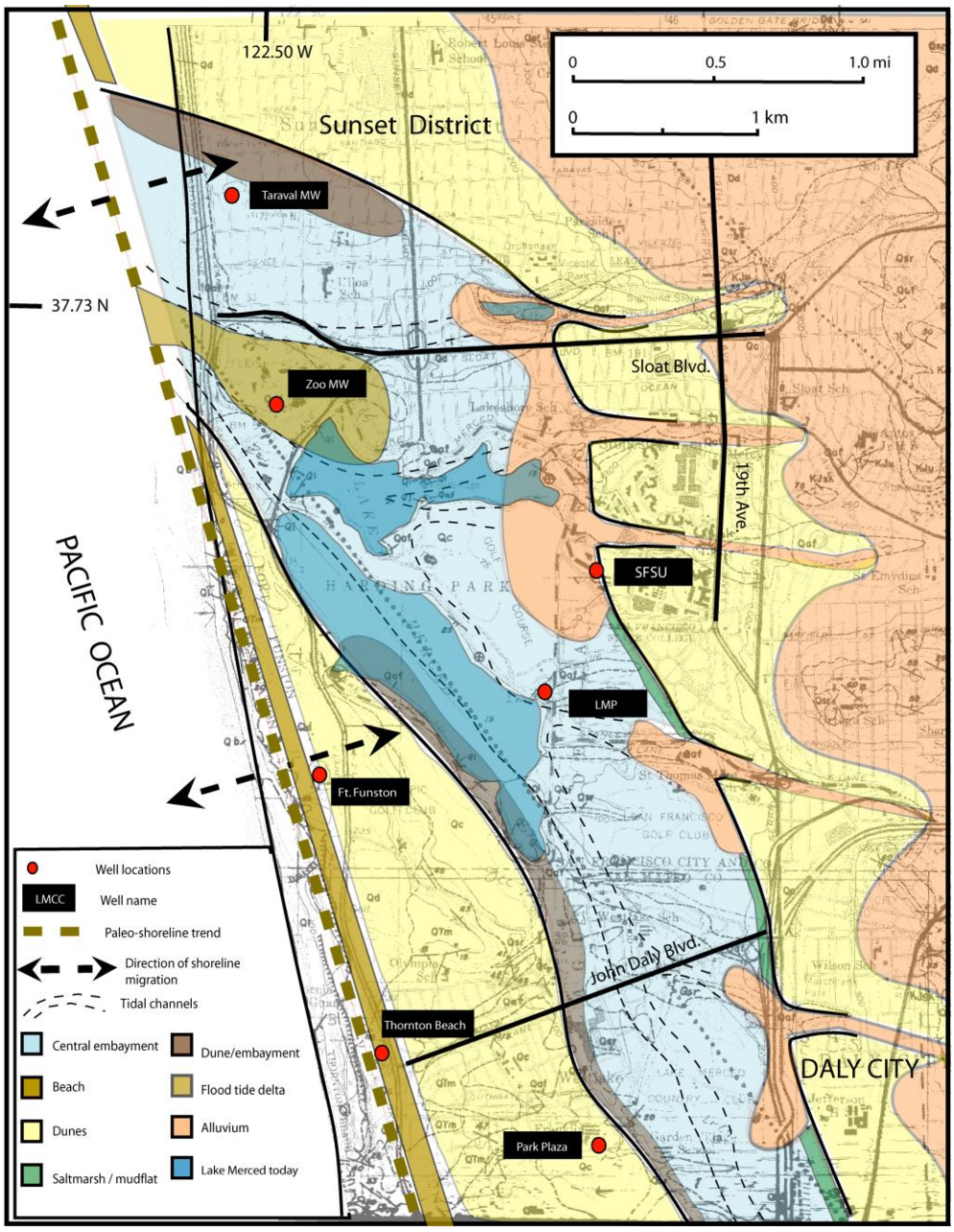

Figure 4. Paleogeographic map of the study area showing a northwest-southeast trending paleo-shoreline and the generalized trend of embayments, which formed during sea-level high stands. Map also shows various depositional environments within the beach/barrier/embayment system. Base map from Bonilla (1971).

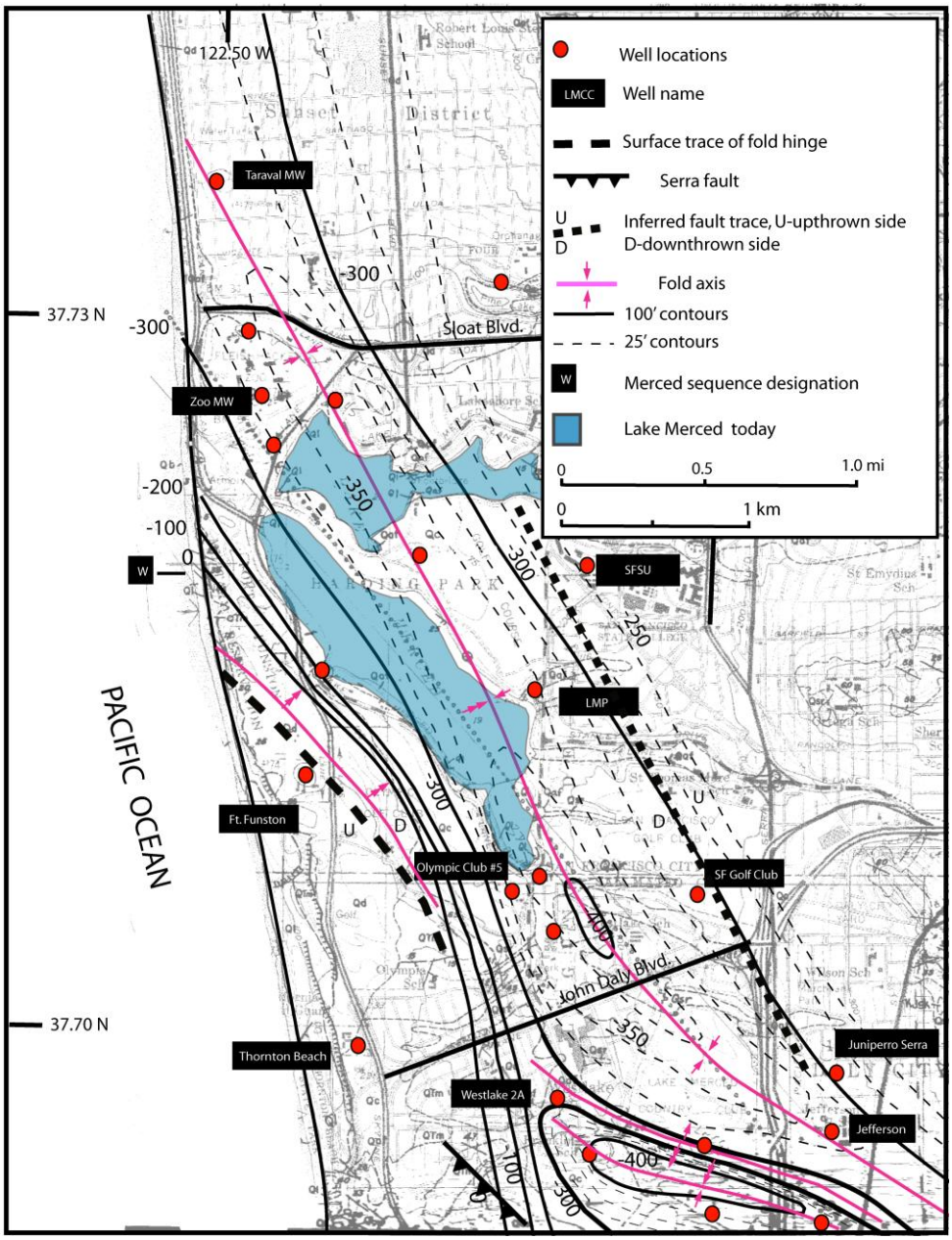

Figure 5. Structure, mapped on the base of Sequence W. Map shows broad northwest-southeast trending syncline, monoclinal fold associated with the Serra blind thrust fault, a structural depression southeast of the Westlake 2A well, and faulting or folding in the eastern part of the study area. Basemap from Bonilla (1971).

MERCED AND COLMA FORMATIONS

Sediments of the Merced and Colma Formations are the primary aquifer-forming strata in the North Westside Basin (Rogge, 2003). The Merced Formation is composed of over 1700 m of poorly consolidated sand, mud and gravel deposited in a tectonically-active, marginal-marine environment. Clifton et al. (1988) delineated over 40 sequences in the northeast-dipping coastal exposures that consist of shelf, nearshore, backshore, embayment and fluvial facies (Plate 1). Shelf facies are predominant in the lower Merced, while terrestrial sediments are more common in the upper Merced (Figure 6). Hall (1965) informally divided the Merced into upper and lower units based on a mineralogy change that occurs within Clifton et al.'s (1988) sequence P. The mineralogy change is characterized by a shift from locally-derived, plutonic, Franciscan minerals to Sierran-derived, plutonic and andesitic minerals. The influx of Sierran sediment is thought to represent the opening of the Golden Gate to Sacramento-San Joaquin (Central Valley) drainage (Sarna-Wojcicki et al., 1985). This change also appears to mark the beginning of a period of more rapid sedimentation that resulted in a shift from primarily offshore deposition to mostly backshore sedimentation (Clifton et al., 1988).

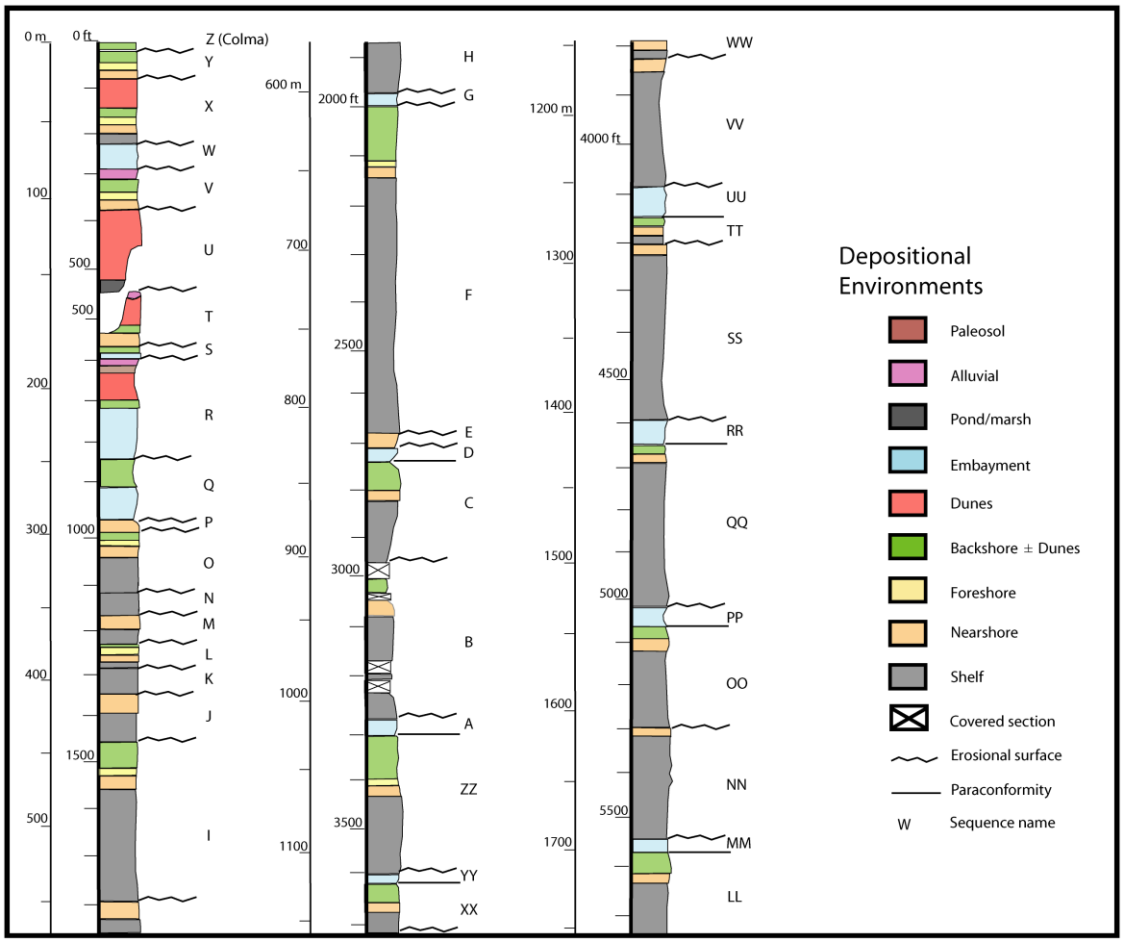

Figure 6. Clifton et al.'s (1988) complete coastal stratigraphic column, showing shelf dominated lower sequences and terrestrial dominated upper units.

Both the lower and upper parts of the Merced are composed of unconformity-bounded transgressive and regressive sequences that likely represent Pleistocene sea-level changes superimposed on a tectonically-subsiding coastline (Clifton et al., 1988). Regressive sequences in the Merced typically prograde from shelf or nearshore to foreshore and backshore environments, whereas transgressive sequences in the upper Merced tend to consist of muddy embayment deposits that grade upward into dune

sand or muddy embayment deposits that then grade upward into sand and gravel of tidal-channel deposits (Hunter et al., 1984).

Structurally, the Merced is bounded to the southwest by the peninsula segment of the San Andreas fault (PSAF) and is cut by the Serra fault (Figure 1; Bonilla, 1971; Yancey, 1978; Brabb et al., 1998; Barr, 1999, Kennedy, 2002). At the base of the coastal section, near the PSAF, beds dip 50° or more to the northeast. In this area, northeasterly dips become more shallow up section, with nearly horizontal strata between Thornton Beach and Fort Funston (Plate 1). Approximately 1 km north of Fort Funston, the beds become steeper, reaching dips of greater than 50° NE along a northeast-vergent propagation fold located above the concealed (i.e., blind) strand of the Serra fault where it intersects the coastal bluffs (Kennedy, 2002).

Approximately 200 m north of where the northeast-vergent fold intersects the coast, there is an angular unconformity between sequences X and Y (Plate 1). Farther north, bedding within the Merced (Y) and Colma (Z) flatten, averaging 20° NE or less (Plate 1; Bonilla, 1971; Clifton and Hunter, 1987; Kennedy, 2002). South of Lake Merced, strands of the Serra thrust system break the surface and place older Merced strata above younger Colma (Figure 1) as well as Franciscan Complex bedrock over strata of the Merced and Colma Formations. (Bonilla, 1971, Yancey, 1978; Brabb et al., 1998; Kennedy, 2002).

The precise age range of the Merced Formation remains uncertain. Hall (1965) and Yancey (1978) assigned to the unit a late Pliocene to Pleistocene age based on a variety of faunal evidence. Clifton et al. (1988) suggested that deposition was restricted to the Pleistocene, also based on an analysis of invertebrate fauna in the Merced and other Quaternary units. The only datable ash bed in the Merced is located in sequence S (Figure 2; Plate 1), 175 m below the top of the section. It has been correlated to the Rockland ash (Sarna-Wojcicki et al., 1985), and assigned a numerical age of ~400 ka based on fission-track dating of zircon grains (Meyer et al., 1991; ages range from 370 ka to 460 ka). More recently, Lanphere et al. (2004) used $^{40}Ar/^{39}Ar$ dating of plagioclase grains and U–Pb dating of zircon grains to constrain the eruptive age of the Rockland ash to between 565–610 ka. Ingram and Ingle (1998) collected 17 samples from 330 to 1670 m below the top of the section and extracted foraminifera shells for $^{87}Sr/^{86}Sr$ dating. Their youngest sample, located in sequence O about 160 m below the Rockland ash, was dated at 590–650 ka, supporting an age closer to 500 ka than to 600 ka for the ash. Similarly, Hall's (1965) mineralogical change in sequence P, located ~125 m below the ash bed, is believed to coincide with the opening of the Golden Gate drainage and the end of deposition of the Corcoran clay in a Central Valley lake about 600 ka (Sarna-Wojcicki et al., 1985). With 125 m between the mineralogical change and the Rockland ash, a difference in age of ~100 k.y. seems likely, but the discrepancy has yet to be reconciled. I have compiled Merced ages in Table 1.

Dated unit	Depth (m)	Sequence	Min. age (ka)	Max. age (ka)
Colma base	3-16	Z	80	130 (a)
Olema Ash	3-16 (?)	Z (?)	55	75 (b)
Rockland Ash	175	S	370	460 (c)
Rockland Ash	175	S	565	610 (d)
Mineralogic change	295	P	~600	~600 (b)
Sr isotope	330	O	590	650 (e)
Sr isotope	515	I	640	700 (e)
Sr isotope	705	F	700	800 (e)
Merced Base	1670	NN	2400	4800 (e)
Merced Base	1750	LL	1500	2000(f)

Table 1. Merced and Colma Formation depth, sequence and age data [(a) Chappell and Shackleton, 1986; (f) Wakabayashi et al., 2004; (d) Lanphere et al., 2004; (e) Ingram and Ingle, 1998; (c) Meyer et al. 1991; (b) Sarna-Wojcicki et al., 1985). (?) Olema ash is contained within a channel deposit inset into sequence Y. Because the channel deposit occupies the same stratigraphic position as the Colma, the ash may be comparable in age to the Colma.

The age of the lower part of the Merced is less certain than the upper part. Ingram and Ingle's (1998) models produced ages of 2.4 Ma (their preferred model) and 4.8 Ma for the base of the Merced. Wakabayashi et al. (2004), based on a reconstruction of basement features along the PSAF, suggests that motion began 1.3 to 2.1 Ma, initiating deposition of the Merced Formation. This idea supports Ingram and Ingle's younger age (2.4 Ma) and because their isotopic data are poorly constrained for the base of the Merced and several 2.4-2.0 Ma regional tephra layers are missing from the formation this younger date may be more accurate. More recent data from the offshore zone, however, suggest that the basal part of the Merced may be equivalent in age to the upper beds of the Purisima Formation and that the lower part of the Merced may have been deposited in an open-coastal environment prior to the initiation of the PSAF

(Ryan et al., 2008). In the "Pleistocene sea level fluctuations related to Merced sequences" section, I discuss the age estimates in the context of Clifton et al.'s (1988) data and my sequence correlations.

The late Pleistocene Colma Formation unconformably overlies variably tilted beds of the Merced Formation (Plate 1). The unit consists of poorly consolidated beach, estuarine, eolian, stream and colluvial deposits that are distributed discontinuously throughout the northern part of the San Francisco Peninsula (Schlocker, 1974). Along the coast, deposits consist of nearshore and backshore deposits while inland the Colma consists of eolian, stream and colluvial deposits (Schlocker, 1974). Coastal bluff thicknesses range from erosional remnants of about 1 m at the south end of Ocean Beach to 13 m at Thornton beach (Yi, 2005). Inland, thicknesses can reach 30 m (Schlocker, 1974; Yi, 2005). Colma Formation strata, which were deposited at sea level, have been uplifted as much as 25 m at the south end of Ocean Beach and 70 m at Thornton Beach (Bonilla, 1971; Kennedy, 2002; Yi, 2005), where strata consist of nearshore to backshore deposits (Plate 1). Overlying and interfingered with the Colma Formation are discontinuous Holocene dune sands, colluvial and alluvial deposits (Plate 1; Bonilla, 1971; Schlocker, 1974).

Schlocker (1974) assigned a late Pleistocene age to the Colma based on the unit's location between the Plio-Pleistocene Merced Formation and Holocene dune sands. Kennedy (2002) identified the Olema ash layer (55-75 ka) within fluvial deposits inset into Merced sequence Y in coastal exposures near Sloat Boulevard in San Francisco (Sarna-Wojcicki, unpublished data). The ash deposits must be younger than sequence

Y and could be older or age-equivalent to sequence Z (Colma Formation). Most recently, Yi (2005), in an effort to better assess Colma uplift rates, dated the unit using the optically stimulated luminescence (OSL) technique. Yi's (2005) results yielded Colma ages that appear to be systematically too young. Given the constraints imposed by the age of the Olema ash and the stratigraphic position and elevation of the Colma, the unit is generally thought to have been deposited during the high stands associated with the last interglacial [oxygen isotope stage 5e, 5c or 5a], between 80 and 130 ka (Figure 7, Chappell and Shackleton, 1986).

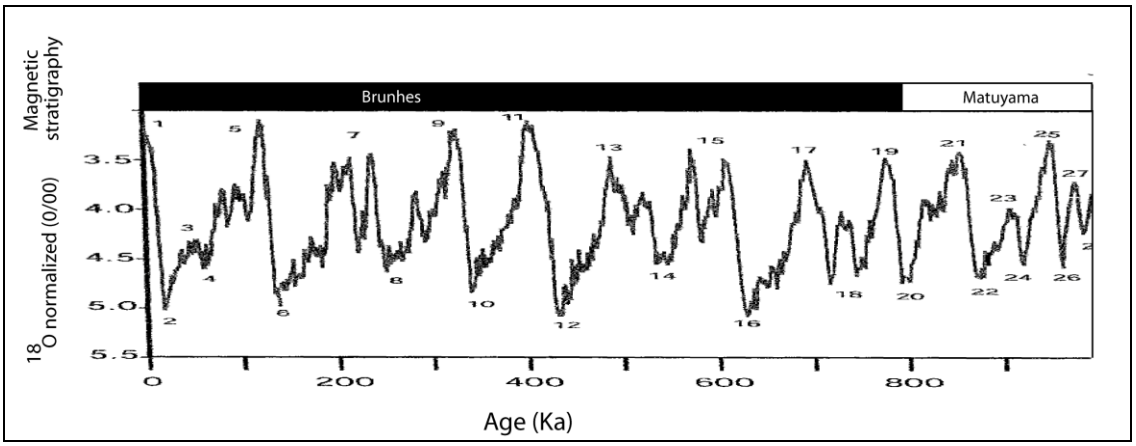

Figure 7. Pleistocene sea level curve showing oxygen isotope stages (numbers 1–27). High stands (odd numbers); low stands (even numbers). Figure adapted from Lisiecki and Raymo, 2005.

.

GEOLOGIC SETTING

The Merced and Colma Formations were deposited during a time of changing tectonic regimes, including initiation of the PSAF and the Serra fault. The next section focuses on the geotectonic setting within which the formations were deposited.

The Merced Formation is exposed in a 3-km-wide, 19-km-long northwest–southeast trending outcrop belt that intersects the coastal bluffs on the west side of the San Francisco Peninsula south of Ocean Beach (Figure 1). The formation is underlain by rocks of the Franciscan Complex and tectonically, the northeast-vergent Serra thrust fault cuts the northern part of the section and the peninsula segment of the San Andreas fault (PSAF) bounds the formation to the southwest (Figure 1).

The unit lies nonconformably on rocks of the Franciscan Complex (Figure 1; Bonilla, 1971; Yancey, 1978; Pampeyan, 1994; Brabb et al., 1998). The Franciscan is the primary bedrock type in the California Coast Range Province, which extends along the coast from north of Santa Barbara in southern California to Oregon (Jennings et al., 1977). This highly deformed unit of late Jurassic to Cretaceous marine sandstone, shale, siltstone, chert and volcanic rocks was folded, sheared and fractured as it was accreted to the continental margin during subduction of oceanic crust (Ring, 2008). Most of the San Francisco Peninsula is underlain by the Franciscan Complex and the unit forms topographic highs, whereas younger sedimentary units like the Merced and Colma Formations have filled in the topographic lows (Figure 1; Bonilla, 1971; Schlocker, 1974; Kennedy, 2002).

The Merced Formation straddles the San Francisco Bay and Pilarcitos structural blocks, which are bounded to the east by the Hayward–Calaveras fault system and to the west by the San Andreas and Pilarcitos faults (Figure 8; Jennings et al. (1977); Jachens and Zoback, 1999). The right-lateral, strike-slip San Andreas fault, which has been active since the early Miocene has over 300 km of cumulative displacement in certain areas and extends over 1000 km, from the Gulf of California north to Point Arena, California (Matthews, 1976; Graham, 1978; Atwater and Stock, 1998). The San Andreas fault system is a relatively linear strand north and south of the Bay Area, but splits into multiple strands approximately 160 km south of San Francisco, and forms a broad 40-km-wide fault zone around San Francisco Bay (Figure 8; Jennings et al., 1977; Jennings et al., 2002). Motion on the eastern side of this zone, within the East Bay fault system, is accommodated by the Hayward–Calaveras system, whereas to the west, long term slip has been distributed on the San Andreas, San Gregorio, Pilarcitos, and Golden Gate faults (Figure 8 and 9; Jachens and Zoback, 1999; Bruns et al., 2002).

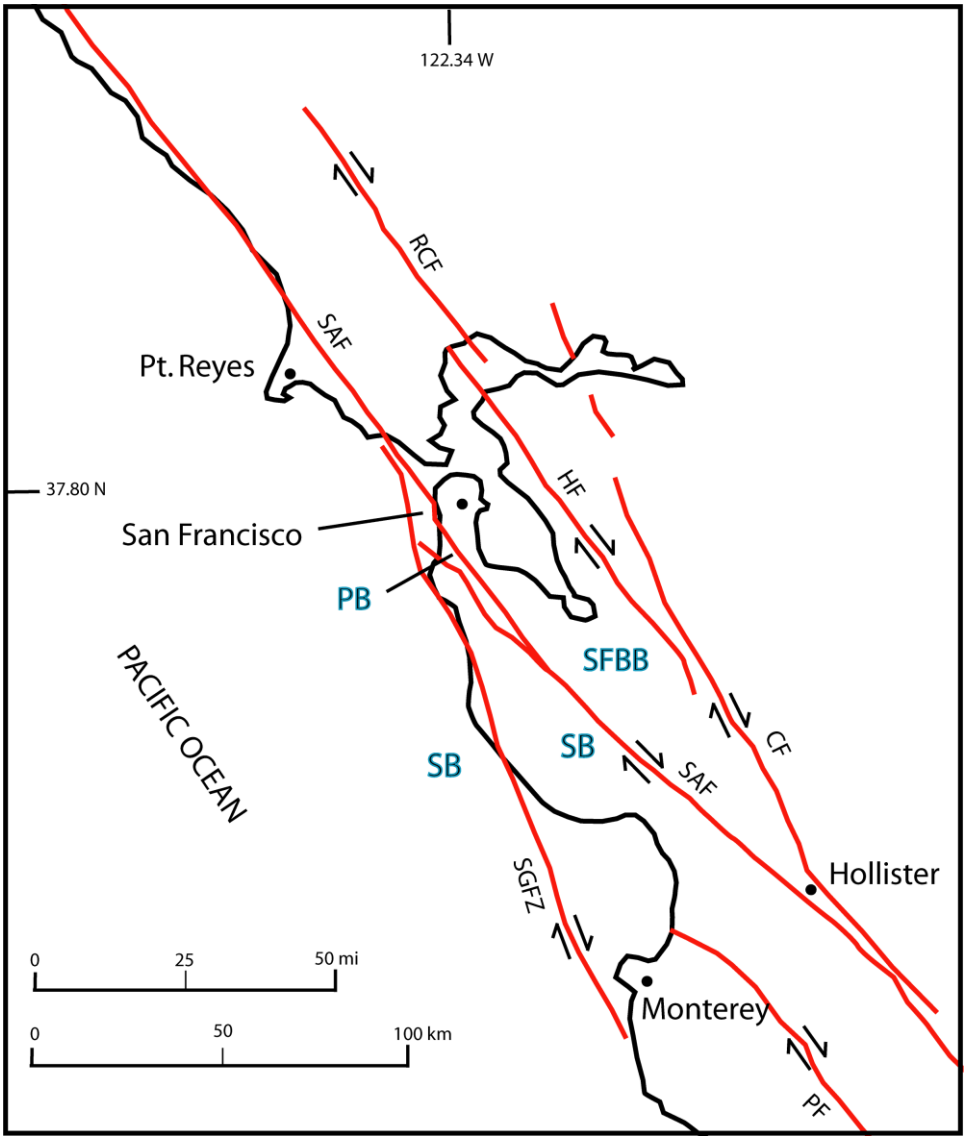

Figure 8. Regional fault map showing the bifurcation of the San Andreas fault (SAF) around the Bay Area and associated structural blocks. San Gregorio fault zone (SFGZ); Calaveras fault (CF); Hayward fault (HF); Pilarcitos Fault (PF); Rogers Creek fault (RCF); San Francisco Bay block (SFBB); San Gregorio block (SB); Pilarcitos Block (PB). Map adapted from Kennedy (2002). Faults adapted from Jennings (1977) and Lajoie (1996).

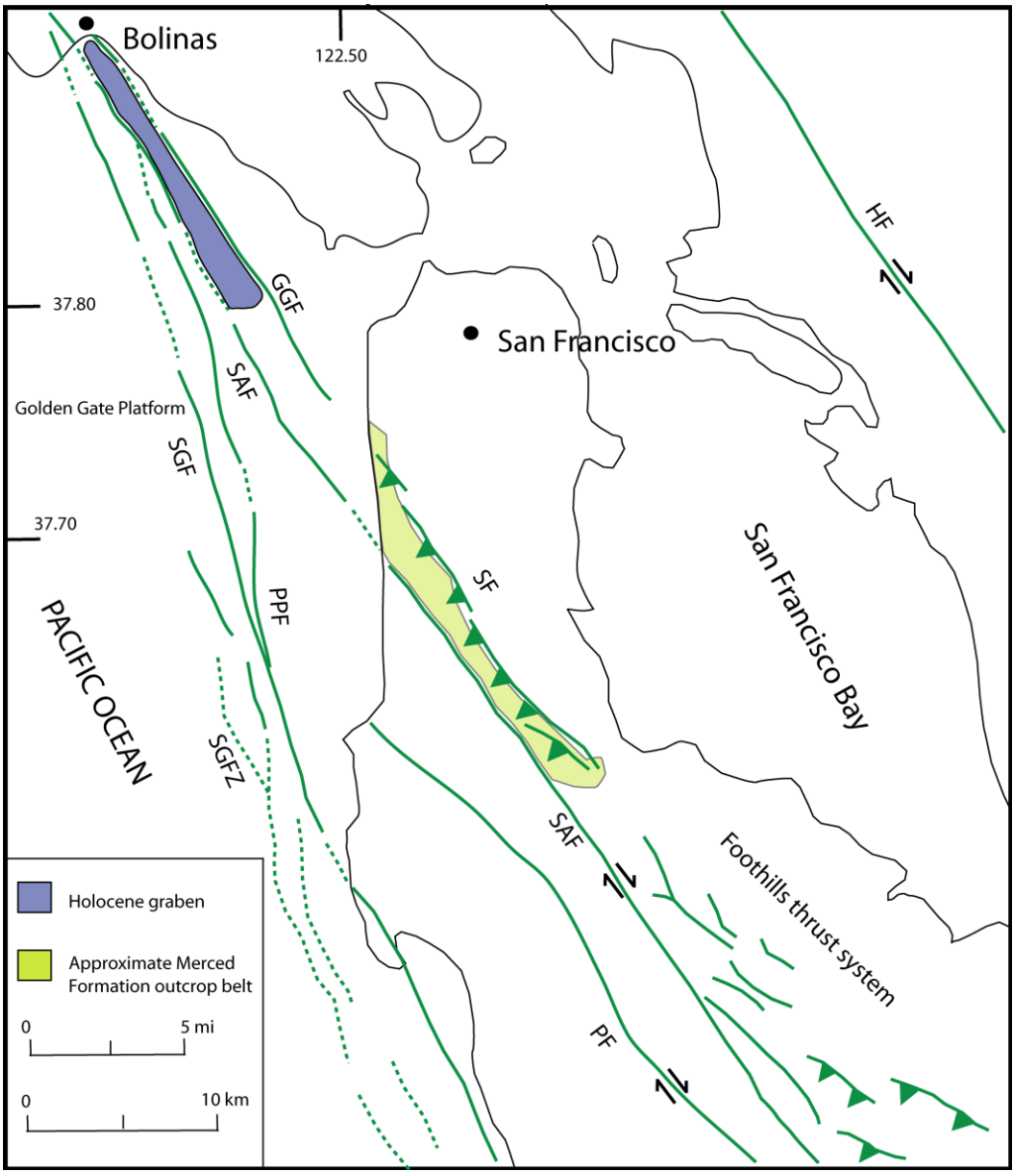

Figure 9. Map showing the spatial relationship between the Foothills thrust system, San Andreas fault (SAF), Serra Fault (SF), Merced Formation and the current depositional basin west of the Golden Gate. Map adapted from Kennedy (2002). Faults adapted from Jennings et al. (2002) and Lajoie (1996). Offshore fault data adapted from Bruns et al. (2002). Golden Gate fault (GGF); San Gregorio fault (SGF); Potato Patch fault (PPF); San Gregorio fault zone (SGFZ).

Using seismicity and aeromagnetic data Zoback et al., (1999) suggest that in the northern most part of the San Francisco Peninsula, the SAF is primarily extensional. However, the uplifted Merced Formation appears to record a transpressional style of deformation that was preceded by transtensional deformation. McLaughlin et al. (1999) note that the Foothills thrust system, which trends sub-parallel and to the northeast of the PSAF in the southern peninsula, records late Cenozoic, northwest-propagating compression (Figure 9; Lajoie, 1996; McLaughlin et al., 1999). Basin-bounding normal faults located in the hanging walls of these structures together with a northwest-younging of Miocene stratigraphy suggest that subsidence preceded uplift (McLaughlin et al., 1999). The Serra fault in the Lake Merced area may be a reactivated normal fault associated with a steep bedrock escarpment beneath Lake Merced. If so, this suggests that the pattern of northwest-propagating subsidence followed by uplift is possibly regional and may explain the deposition and subsequent uplift of the Merced Formation.

Strike-slip fault systems are often characterized by bends or steps that create localized areas of subsidence or uplift (Sylvester, 1988). Aeromagnetic and seismic data acquired on the offshore Golden Gate Platform suggest the SAF bends eastward and motion may be transferred 3 km east to the Golden Gate fault (Figure 9; Jachens and

Zoback, 1999; Bruns et al., 2002). Additionally, seismic data acquired by Bruns et al. (2002) indicate that the active depositional basin on the Golden Gate Platform is located approximately 12 km northwest of the Golden Gate, between strands of the San

Andreas and the Golden Gate faults (Figure 9). Wakabayashi (2004) suggested that the Merced, whose coastal outcrops are located 19 km southwest of this active basin, was deposited in a similar pull-apart basin that has migrated northwest to its present position, leaving in its wake a transpressional environment that has uplifted the Merced Formation. A more recent study by Ryan et al. (2008), however, suggests that the Merced may be a dismembered part of a larger, open coastal basin, with sediments deposited between the San Gregorio and San Andreas faults, and that a right step to the Golden Gate fault is not required to explain its deposition.

METHODS

Primary Data

To develop my subsurface model, the primary data I used were geophysical logs (resistivity, spontaneous potential—SP, and gamma), drillers' lithologic logs, well cuttings, outcrop stratigraphy and surface mapping. I first collected paper copies of geophysical logs and drillers' lithologic logs within the study area, scanned all paper copies and imported them into the software package LogPlot 2005 where I uniformly scaled them to 1 inch =50 ft (15 m) (Appendix A). I obtained digital Log ASCII Standard (LAS) data for six wells and also used LogPlot 2005 to plot these curves at the same scale as the scanned data.

I then integrated lithologic data with the uniformly scaled logs. Accompanying most paper copies of geophysical logs were drillers' notes describing the sediment types encountered during the drilling process. Drillers' notes tend to vary in their degree of detail, so I used the geophysical data, well cuttings, and my interpretations of sediment types in nearby wells to organize and create meaningful sedimentologic packages for each well. I used these sedimentologic packages to create graphic stratigraphic columns that I paired with the geophysical data. The result is a highly usable, integrated, uniformly scaled package of geophysical and lithologic data readily usable for well correlations (Appendix A).

To augment the geophysical and drillers' sedimentologic data, I studied coastal outcrops and examined well cuttings for eight wells in the study area (Kirkham, Ortega, Taraval, Zoo MW, Lake Merced Pump Station, Daly City Junipero Serra, Daly City Park Plaza, Thornton Beach). I studied the Merced Formation outcrops using the stratigraphic framework developed by Hunter et al. (1984), paying special attention to sequence boundaries and vertical and lateral stratigraphic changes (Figure 2 and Plate 1). I then compared the coastal sediments to the well cuttings. When I received the cuttings they were packaged in plastic bags collected at ten-foot (3 m) intervals. To better view the vertical changes in sediment type and to compare the cuttings to the coastal sediments, I created a pseudo-core by placing a mixed sample for each bagged interval into subdivided tackle boxes labeled by depth interval (Figure 10). Next, using a hand lens, binocular microscope, grain-size comparator and the grain-sorting charts of Compton (1985), I qualitatively described the color, grain size, angularity and

sorting of the sediments and incorporated this information into the graphic lithologic columns using LogPlot 2005. Also, after organizing the cuttings, I compared them to their respective geophysical logs to observe how resistivity, SP and gamma responses compared to local sediment type.

Initial Correlation Strategy

To begin correlating wells I used geophysical data, well cuttings, drillers' notes, and outcrop and surface mapping to divide the apparent sedimentary sequences in each well into lithologic packages that could be compared to the sequences delineated by Hunter and Clifton (1982) and exposed in the coastal bluffs (Figure 2 and Plate 1). I focused on correlating sequence boundaries because they tend to be controlled by eustatic or relative sea-level changes and provide good time lines. Within each sequence, sediment type varies depending on the depositional environment. For example, while coarse-grained nearshore sediments were being deposited at the location of current coastal exposures, fine-grained embayment sediments were being deposited farther inland, behind a barrier (Figure 4). My goal was to delineate the sequence boundaries and to interpret sediment changes within each sequence in the context of reasonable lateral facies variations.

I developed the initial correlation strategy using two wells: the Lake Merced Pump Station (LMP) and the most recently drilled monitoring well in the zoo area (Zoo MW) (Figure 3). I started with these wells because I assumed that strata between them

Figure 10. Photograph of well cuttings organized in tackle boxes to create a "pseudo-core" to better observe vertical sedimentologic changes.

would be less deformed than strata located closer to the Serra fault. Additionally, I had well cuttings for both of these wells and anticipated that the 6000 ft (1900 m) of lateral separation would demonstrate how facies change from the nearshore (Zoo MW) to the backshore (LMP) environment.

To identify sequence boundaries using these wells, I first assumed a minimum Colma Formation (sequence Z) thickness of 40 ft (12 m) at the top of the LMP well (Kennedy, 2002; Bonilla, 1971). This was based on a well-head surface elevation of approximately 40 ft (12 m), and previously mapped Colma Formation sediments from the ground surface down to the water surface of Lake Merced. Using this minimum Colma thickness, I worked from the top downward, attempting to match Hunter et al.'s (1984) sequence thicknesses on the coast to the LMP geophysical and lithologic logs. Using this technique, I interpreted the bottom sequence in the LMP well as "S" and identified overlying sequence boundaries, considering the lateral facies changes that are likely between the coastal exposures and the LMP well (Appendix B).

In the Zoo MW well, I designated the uppermost fine-grained unit as sequence Y. In this well, I then worked from the top downward, attempting to match Hunter et al.'s (1984) unit thicknesses to the Zoo MW geophysical and lithologic logs. I again interpreted the basal unit as sequence "S" and identified overlying sequence boundaries considering the likely lateral facies changes between the coastal exposures and the well (Appendix B). Using the sequence correlations between the LMP and Zoo MW wells, I developed a paleogeographic model and expanded correlations among coastal exposures and other wells.

Fold Construction

Merced and Colma Formation strata in the study area are uplifted by the blind Serra thrust fault and form a northeast-vergent monoclinal fault-propagation fold that intersects the coastline approximately 1 km north of Fort Funston (Figure 1; Plate 1; Kennedy, 2002). In my cross sections I constructed folds and projected depths to sequence boundaries using the coastal stratigraphy of Hunter et al. (1984) and Clifton et al. (1988), and the bedding attitudes mapped and compiled by Kennedy (2002). To construct the fold along coast-parallel cross section A-A', I used Clifton et al.'s (1988) coastal stratigraphy projected inland to the Fort Funston well log and then projected the coastal fold attitudes, as mapped by Kennedy (2002), inland to the line of cross section (Appendix C). Along coast-oblique cross section E-E', I constructed the fold using Clifton et al.'s (1988) coastal stratigraphy projected to the Fort Funston well log and constrained the fold using a dip attitude of the Rockland ash exposed in the Olympic Club and mapped by Kennedy (2002) (Figure 3; Appendix C). To the south, along coast-oblique cross section F-F', I again used the coastal sequences of Clifton et al. (1988), but in this location I projected to the Thornton Beach well and used Rockland ash bedding attitudes located approximately 0.8 km inland to constrain the fold and to project beds to depth (Figure 3; Appendix C). All mapped bedding attitudes were adjusted for apparent dips and vertical exaggeration on the cross sections.

RESULTS AND DISCUSSION

In this study I used subsurface and surface data to interpret the depositional environments of sediments observed in each well and to correlate these sediments among wells and with coastal Merced Formation exposures. I show the results of these interpretations and correlations in six cross sections (Plates A–F), which I have used to develop models for basin paleogeography and structure and to map the distribution of units that form aquifers and aquitards in the subsurface. In the following sections I first discuss the Merced basinal structure, followed by the sedimentology and stratigraphy of the relevant aquifer-forming units and my basis for correlating each sequence and interpreting the lateral facies variations. I then examine the location and extent of the primary aquifers and aquitards and the relationship between my interpretations and recently analyzed water-quality data. Finally, I discuss the external controls on sedimentation in the basin.

Basinal Structure

Interpreting the sequence correlations and the basinal structure was an iterative process, in that the correlations helped to interpret the structural features and, in turn, the structural features helped to correlate the sequences. Deformation of the basin has created abrupt changes in dip and a complex arrangement of once-horizontal strata that hampered the correlation process. Interpretations were further complicated by the

abrupt facies changes that are a natural product of deposition in coastal environments in active tectonic settings. Although the sedimentary correlations were essential to understanding the basinal structure, I first present my structural interpretations so that the subsequent correlations can be better understood. In this section, I explain how the structures associated both with the Serra fault and an unnamed fault or fold in the eastern part of the study area appear to have deformed sedimentary sequences.

Based on my structural model, the blind thrust associated with the Serra fault has differentially folded the Merced Formation in the study area, and uplifted it as much as 800 ft (240 m) (Figure 5; Plates A and E). The uplifted strata drape over the blind thrust, forming a northwest–southeast trending escarpment in the Olympic Club (Figure 5; Plates E and F). These beds become abruptly sub-horizontal eastward beneath Lake Merced and rise gently eastward to form a broad northwest–southeast-trending syncline whose uplifted western and eastern limbs appear to open and flatten northward (Figure 5).

The northwest–southeast-trending fault-related escarpment in the Olympic Club appears to terminate to the south near John Daly Boulevard. However, there is another escarpment approximately 4000 ft (1250 m) to the southwest, that may be associated with the Serra fault (Figure 5). In the subsurface, there appears to be a structural depression east of this southern escarpment and southeast of the Westlake-2A well (Figure 5, Plates D and F). North of this depression, between the southern escarpment and the Olympic Club escarpment strata are uplifted but less so than they are above the

blind thrust (Figure 5; Plates E and F). This may be a result of being between fault strands rather than directly above the thrust.

In the eastern part of the study area there appears to be either faulting or very abrupt folding sub- parallel to the Serra fault (Figures 5 and 11). This deformation has uplifted strata to the northeast and is most visible along cross section D-D' (Plate D), where sequence W is uplifted approximately 100 ft (30 m) to the northeast, between the SFSU #2 (northeast) and LMP (southwest) wells. To the southeast, along cross section F-F' (Plate F), there also appears to be approximately 100 ft (30 m) of offset between strata in the Daly City Jefferson and Vale wells (Figure 11 and Plate F). The position and trend of the proposed fault is not well constrained by well logs. However, the structure may be related to a broad southwest-facing escarpment expressed on Harding Park golf course, just south of the east side of Lake Merced's north arm (Caskey, SFSU, pers. Comm., 2008).

Depth to bedrock data for the North Westside Basin provides additional information about the basinal structure (Figure 12). The Franciscan bedrock surface slopes gently westward beneath Lake Merced, and abruptly steepens near the center of the lake to form a west-facing subsurface escarpment. Farther west, the basement surface slopes less steeply and reaches a depth of ~3500 ft (1070 m) at the location of the present-day coastline. I interpret the west-facing bedrock escarpment as a concealed normal fault that was likely active during the deposition of the Merced Formation and was a primary tectonic control on basinal subsidence.

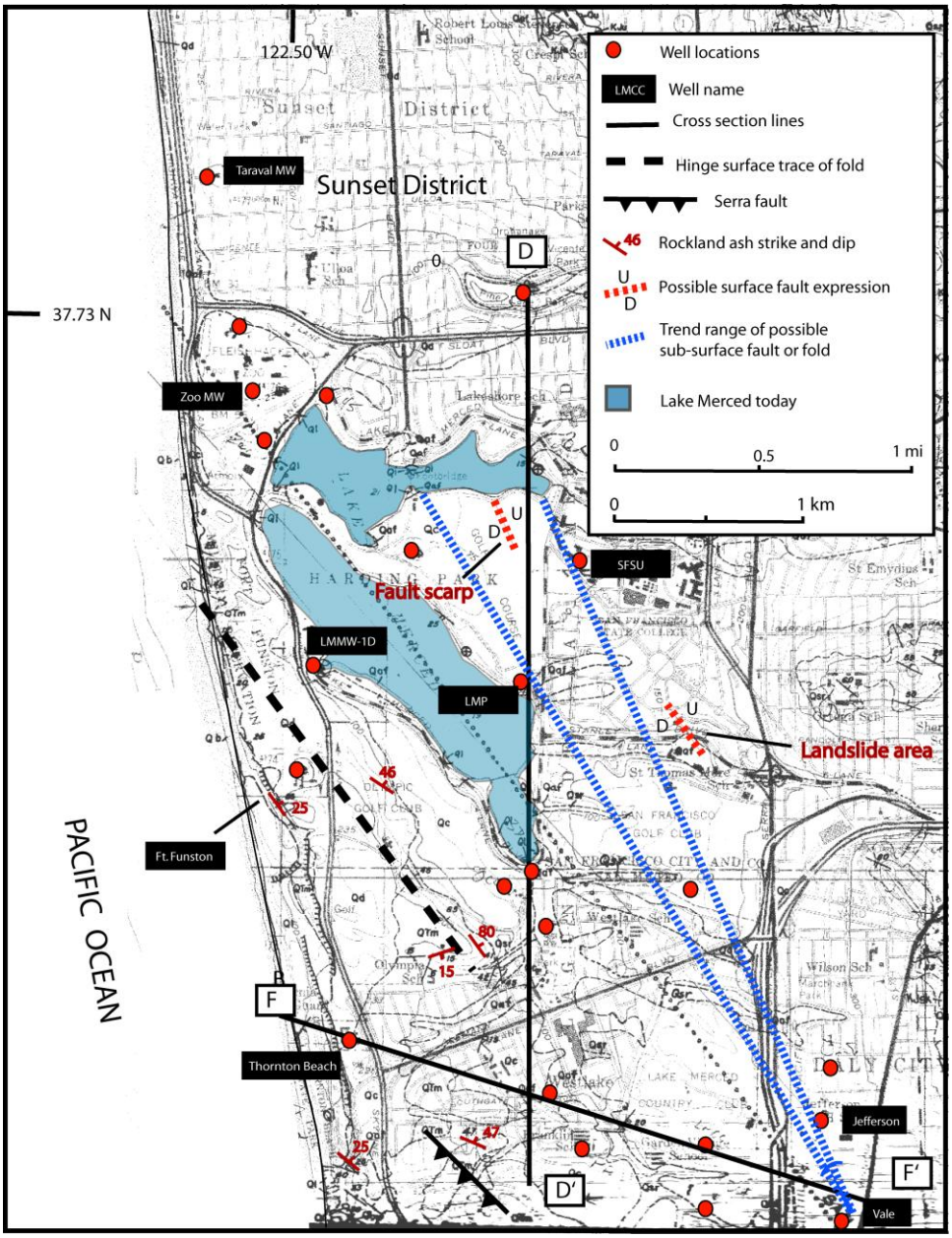

Figure 11. Possible range of subsurface fault trace based on interpreted displacement between Jefferson and Vale wells in the south, northward to displacement between LMP and SFSU wells. Figure also shows possible surface expressions of faulting within and near the fault trace range.

West of the basement escarpment the entire sedimentary succession of the Merced Formation is preserved, whereas to the east of the escarpment only sequences S through Z are preserved (Plates 1 and A). The trend and position of the bedrock escarpment corresponds somewhat closely with the inferred trace of the Serra fault. It is therefore possible that the Serra fault is a reactivated normal fault, at least locally. The transition from normal to thrust motion could thus reflect the change in tectonic stresses as this area evolved from transtenssional to transpressional regimes. Seismic data collected from the offshore zone (Zoback et al., 1999; Bruns et al., 2002; Ryan et al., 2008) provide further evidence for abrupt changes between extensional and compressional tectonism along the coast. In summary, the east-facing surface escarpment formed by a fault-propagation fold over the blind Serra fault appears to be located over the west-facing basement escarpment formed by earlier syndepositional normal faulting during the deposition of the Merced Formation (Figures 5 and 12; Plates E and F).

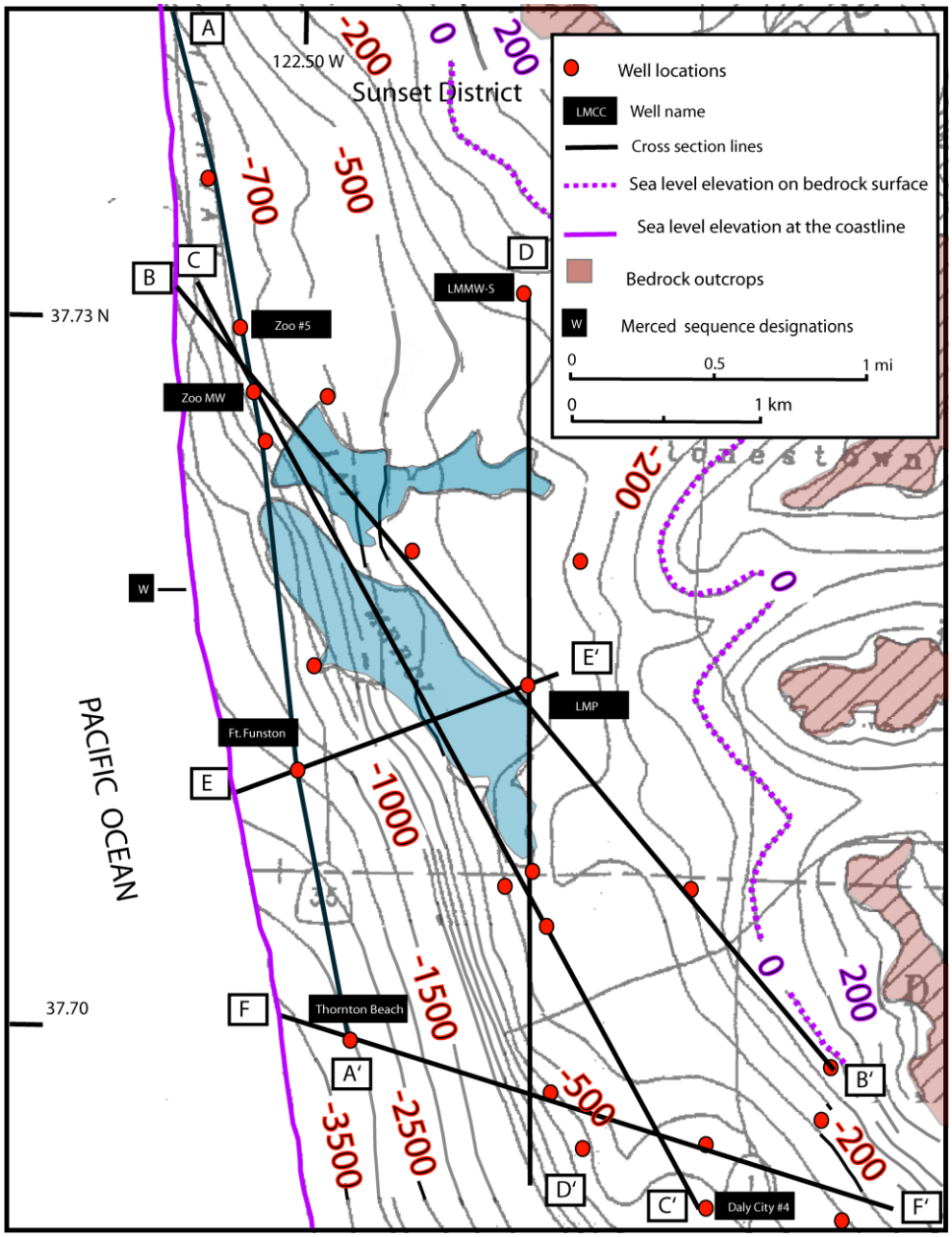

Figure 12. Generalized bedrock surface map adapted from Phillips et al. (1993). Contour interval is 100 ft northwest of bedrock escarpment and 500 ft to the southwest. This map is meant to show the location of bedrock escarpment beneath the Lake Merced area and is not meant to serve as a precise bedrock surface map. Some depths contoured by Phillips et al. (1993) do not coincide with the well data used in this study.

Sedimentology and Stratigraphy: Basis for Sequence Correlation

In the following sections, I describe the sedimentology and stratigraphy of the relevant aquifer-forming strata exposed in the coastal bluffs, as described by Clifton et al. (1988) and Hunter et al. (1984). I explain the basis for correlating each coastal sequence to the wells located closest to the exposures (wells at Fort Funston, Zoo MW and Thornton Beach) and for correlating the sequences in the Fort Funston and Thornton Beach wells across the fault propagation fold associated with the Serra blind thrust fault to the east (Figure 3). To correlate sequences exposed in coastal outcrops to the Fort Funston and Thornton Beach wells, I first used the elevation and bedding attitudes of units in the bluffs and projected the beds to the well locations, while attempting to maintain unit thickness. Next, I attempted to correlate the sedimentology of the coastal exposures to borehole sequences using electric log response (e.g., resistivity), my observations of well cuttings, and drillers' lithologic descriptions. I then used inland bedding attitudes of the Rockland ash near sections E-E' and F-F' (Plates E and F; Figures 3 and 11; Appendix C) to constrain fold shape and to project beds to the sequences I designated in the Lake Merced Pump Station and Westlake-2A wells (Figure 3).

Sequence S and correlation explanation

In this section I describe sequence S and explain how I used this unit as a basis for correlating coastal exposures with the Fort Funston and Thornton Beach wells, and how I used the unit as a basis for correlating the Fort Funston and Thornton Beach wells to inland locations east of the Serra fault.

Sequence S is exposed at beach level just north of Fort Funston at the Daly City storm-water outlet (Plate 1), and the unit increases in elevation to the south. Large-scale landslides have disrupted large areas of the coastal cliffs between Fort Funston and Thornton Beach and have locally concealed the sedimentary sequences. At Thornton Beach, in-situ sediments are again visible in the cliff face. In this area, sequence S has an elevation of about 100 ft (30 m) (Plate 1). Sequence S consists of a shallowing-upward sequence of embayment sediments overlain by backshore eolian sediments (Figure 2; Hunter et al., 1984). The embayment sediments are highly bioturbated muddy sand and the eolian sediments are fine sand with climbing-adhesion-ripple structures (Hunter et al., 1984) and bioturbation by hooved animals. A white vitric ash, known as the Rockland ash bed (Sarna-Wojcicki et al., 1985) lies near the top of sequence S and is interpreted as an air-fall ash because of its relative purity (Hunter et al., 1984). The Rockland ash is the only distinctive marker bed within the entire Merced Formation, and its age is estimated at ~400–600 ka.

Basis for correlating coastal exposures to the Fort Funston well

In the bluffs just below the Fort Funston viewing platform, sequence S is exposed at an elevation of approximately 100 feet (30 m) (Plate 1). My pick for sequence S in the Fort Funston well log is an approximately 30 ft (9 m) thick gray, silty-clay sediment package with low resistivity values that increase upward (Appendix B). The base of this unit is located at an elevation of -44 ft (-13 m). I assume that the coastal bluff exposure of S has a 25° NE dip, based on a mapped bedding attitude approximately 500 ft (150 m) south of cross section E-E' (Figure 3). Using this attitude, I projected from the coastal exposure to the well, with no apparent dip adjustment on section E-E' (Plate E) because the bedding strike coincides with the trend of the cliff face. Using a continuous 25° NE dip, the projection of the sequence's base intersects the well at an elevation of approximately -180 ft (-55 m), which is over 200 ft (70 m) below the borehole target (Plate E; Appendices B and C). To correlate the coastal exposure to my target, I allowed the dip of S to decrease in the subsurface to approximately 13° and intersect the target at an elevation of -54 ft (-16 m). The surface trace of the monoclinal fold hinge above the Serra blind thrust is approximately 80 m east of the well (Figure 3) and the fold has probably uplifted stratigraphic units inland, relative to the coastal exposure. Using this geometry, I was able to tie the outcrop to the well log, create a cross section and build up the sequences above and below sequence S (Plate E). *I used this method for all subsequent outcrop to well correlations at the Fort Funston location.*

Basis for correlating coastal exposures to the Thornton Beach well

In the Thornton Beach area, the base of sequence S is located at an elevation of approximately 145 ft (46 m) in the coastal bluffs and is overlain by approximately 40 ft (13 m) of Colma Formation, which caps the bluff (Plate 1). In the Thornton Beach well log, my pick for sequence S is an approximately 30 ft (9 m) thick, gray, sticky clay with traces of medium sand, which has a low resistivity kick and values that increase upward (Plate F; Appendix B). I assumed a 25° NE dip, based on a bedding attitude mapped approximately 1600 ft (500 m) to the south (Figure 3). In cross section F-F', I corrected this to a 13° apparent dip because the strike of the beds is not parallel to the cliff face. An orthogonal projection from the coastal bluff to the well (Appendix C) intersected the well at an elevation of 125 ft (38 m), which is about 10 ft (3 m) below the target elevation (Plate F; Appendix B). Assuming the true dip of S may be shallower than 25°, which is possible given that Merced bedding attitudes appear to be relatively flat in this area, I was able to tie the outcrop to the well log (Plate F). *I used this method for all subsequent outcrop to well correlations at the Thornton Beach location.*

Basis for correlating Fort Funston and Zoo MW wells

North of Fort Funston, I extended sequence S to the Zoo MW well by projecting the fold axis and bedding attitudes mapped by Kennedy (2002) in the coastal bluffs onto cross section A-A' (Plate A). I did this by projecting Kennedy's (2002) fold axis offshore and averaging the bedding attitudes of units exposed in the coastal bluffs at distances of 0–40 m (0-130 ft), 40–80 m (130-260 ft), and 80–120 m (260-390 ft) away from the fold axis. This method produced a model for the shape of the monoclinal fold as it trends highly oblique to A-A' (Plate A). I pulled the stratigraphic units through the Fort Funston well, and sequentially shallowed the dip northward towards the Zoo MW well based on the averages calculated from the coastal outcrop. *I used this method for all subsequent correlations between Fort Funston, the coastal bluffs and the Zoo MW well.* My pick for S in the Zoo MW well was an approximately 50 ft (15 m) thick, gray, poorly-sorted, sub-angular to angular, clayey sand and gravel at an elevation of -615 ft (-188 m) at the base of the well. This unit is overlain by a reddish-brown, medium to coarse, moderately sorted, sub-angular to rounded sand (Plate A; Appendix B). The base of S shows a positive, resistivity kick, corresponding to the clayey sand and gravel that decreases upward into the reddish brown sand.

Basis for correlating Fort Funston to inland wells

The northernmost outcrops of the Rockland ash (sequence S) are located in the Olympic Club, about 1600 ft (480 m) southwest of the Fort Funston well (Figure 3). The ash, which was exposed in a temporary quarry (Kennedy, 2002), dips 46° NE in this area, which lies within the forelimb of the fault propagation fold associated with the Serra fault. To construct the fold along cross section E-E' (Plate E) and constrain correlations between the Fort Funston well and inland wells, I projected this bedding attitude along strike to cross section E-E', adjusted for apparent dip, and built up sequences above and below sequence S, while attempting to maintain constant unit thicknesses (Plate E; Appendix C). I then used my sequence designations in the LMP well (Plate E; Appendix B) to constrain sequence boundaries as I extended them eastward under Lake Merced. I used the LMP well as a constraint because I had well cuttings and the log response was detailed. Using this method I was able to construct the fold shape, constrained by the position and attitude of the Rockland ash. A significant result was that sequence S appears to lap onto the Franciscan bedrock surface just east of the LMP well (Plate E). *I used this method as the basis for all subsequent correlations from the Fort Funston well, across the surface trace of the fold hinge to inland well locations.*

Basis for correlating Thornton Beach to inland wells

To the south, near Thornton Beach, there are several mapped exposures of the Rockland ash—two on the north side of cross section F-F' (Figure 3) and one on the south side (Figure 3; Kennedy, 2002). I first used the 47° NE bedding dip located approximately 1250 ft (380 m) southwest of the Westlake-2A well because this attitude is closer to the cross section than the two attitudes located approximately 3000 ft (960 m) northwest of the well. I first projected the 46° NE attitude, downdip to cross section F-F', to estimate the depth to unit S at that location along the cross section (Plate F; Appendix C). This projection initially intersected the line of section at an elevation of -721 ft (-219 m). If S lies at this depth, additional folding would be needed to bring the unit up to the elevation I picked in the Westlake-2A well (Plate F; Appendix B). Since there is no topographic evidence of a secondary northwest–southeast-trending fold similar to the one in the Olympic Club, and because the bedding attitudes north and south of cross section F-F' indicate that cross section F-F' may be along the axis of a syncline, I suggest that the 46° NE northeast dip shallows at depth (Figure 3). Therefore, I decided to use the subsurface elevation I designated for S in the Westlake-2A well (Appendix B) to back-calculate an "average" true dip from for the ash exposure. This yielded an "average" true dip of 31°, that when projected orthogonal to the line of cross section, intersects F-F' at an elevation of -300 ft (-90 m). From the topographic break in slope shown on Plate F, which I interpret as a possible surface trace of a fold hinge (Figure 3), I first placed sequence S at the 300 ft (90 m) depth described above, and from this location I projected the unit up-dip to where S

extends across the coastal bluff (Plate F). I then projected down-dip through the Westlake 2-A well at the target elevation of -492 ft (-150 m), where there is an approximately 30 ft (9 m) thick gray sand, with a small positive resistivity kick at 650 ft (200 m), indicating that the finer grained embayment muds may not have extended to this location (Plate F, Appendix B). *I used this method as the basis for all subsequent correlations from the Thornton Beach well eastward to inland well locations.*

Based on the correlations described above and other inter-well correlations not described here, it appears that from the coastal exposures of S, the embayment facies extends north and east in the subsurface to where it laps onto the bedrock surface (Plates A–F). To the southeast it appears that the embayment facies transitions to sandier sediment near the Westlake 2A well (Plate F). Coarse-grained sand and gravel found in sequence S in the Zoo MW well indicate that this area may have been a tidal channel or embayment inlet that graded eastward into the more typical embayment sediments of silty sand and mud (Plates A–C).

Sequence T and correlation explanations

Sequence T is exposed at beach level, approximately 625 ft (190 m) north of the Daly City sewer outlets (Plate 1). It rises in elevation to the south, intersecting the top of the bluffs below the Fort Funston viewing platform, where it is overlain by Holocene dune sand (Plate 1). Like S, sequence T is disrupted to the south by the large landslide

complex between Fort Funston and Thornton Beach. Hunter et al. (1984) interpreted T as a regressive sequence approximately 115 ft (35 m) thick consisting of nearshore sand and gravel at the base overlain by foreshore and backshore sand (Figure 2). The backshore deposits contain ephemeral pond deposits with mammoth footprints (Hunter et al., 1984). These sediments are overlain by eolian sand that includes a series of paleosols.

My pick for sequence T in the Fort Funston well is an approximately 70 ft (21 m) thick sediment package consisting of dark, greenish-gray sandy silt overlain by a dark gray silty-clay with shells (Plate E; Appendix B). The log response shows an upward increase in resistivity, followed by a low resistivity spike coinciding with the base of the silty-clay. The target's basal elevation in the borehole is 56 ft (17 m), and using the method described above for sequence S, I tied the coastal exposure to the well log.

North of Fort Funston, I correlated sequence T to the Zoo MW well by projecting the fold axis and bedding attitudes mapped by Kennedy (2002) in the coastal bluffs onto cross section A-A'. My pick in the Zoo MW is an 80 ft (24 m) thick package of gray sand and gravel with shells at an elevation of -565 ft (-172 m) (Plate A; Appendix B). This unit has a negative resistivity inflection at -565 ft (-172 m) elevation, increasing-upward values followed by another negative deflection at 570 ft. / 174 m, and increasingly positive values at the sequence's top (Plate A, Appendix B).

From Fort Funston, I correlated sequence T across the large monoclinal fold using the method described for sequence S. Using the bedding attitude of the northernmost ash

and my sequence boundary pick in the LMP well, I built sequence T above S, while attempting to maintain unit thicknesses (Plate E). I extended T eastward beneath Lake Merced to my target in the LMP well, which is a 70 ft (21 m) thick package of clay, clayey-sand, sandy-clay and sand sediment marked by a relatively low resistivity inflection at an elevation of -550 ft (-170 m), a change upward into blocky, higher resistivity values and an upper low-resistivity interval (Plate E, Appendix B).

At Thornton Beach, sequence T is not visible in the cliff face and the Colma Formation unconformably overlies sequence S (Plate 1). Based on surface mapping (Bonilla, 1971; Kennedy, 2002), it appears that the Colma (sequence Z) is the uppermost unit in the well. Merced strata dip toward the NE in this area and so it is likely that sequence T is present in the subsurface east of the well (Plate F). Based on my subsurface projection of S along F-F', I extended T over S, while attempting to maintain unit thickness. I then projected T up-dip to the west, toward Thornton Beach, and down-dip to the Westlake-2A well. My up-dip projection brought T into the coastal bluffs, where it appears to have been eroded and subsequently overlain by Colma deposits (Plate F). Down-dip, my pick in the Westlake well is an approximately 80 ft (24 m) thick unit consisting of a shell-bearing, gray sand and clay, overlain by clay and sand at an elevation of -492 ft (150 m) (Appendix B). The log response for this interval shows a relatively high resistivity coinciding with the basal shelly sand and clay, followed by a low resistivity spike at the clay and then a high resistivity kick at the capping sand (Plate F, Appendix B).

Based on these correlations and other inter-well correlations not described, the nearshore sediments of the coastal exposure appear to grade laterally north, east and southeast into silty sand and mud that I interpret as embayment deposits formed behind a coastal dune field (Figures 4 and 13; Plates A, B, C, D, E and F). As during the deposition of sequence S, there may have been a tidal channel or inlet in the zoo area, based on shell-bearing, gravelly clay in the Zoo MW well. The gravelly clay transitions eastward into sandy clay in the LMP well, which may have been located in a less energetic central part of the embayment or a peripheral tidal flat/salt marsh environment (Figures 4 and 13; Plates B and C).

Sequence U and correlation explanations

Sequence U is exposed at beach level approximately 1500 ft (457 m) north of the Daly City sewer outlets, at the "south channel" of Kennedy (2002) (Plate 1). The unit rises in elevation to the south, intersecting the top of the cliff face below the Fort Funston viewing platform where it is overlain by Holocene dune sand (Plate 1). Hunter et al. (1984) interpreted U as a regressive/transgressive sequence with an overall thickness of approximately 200 ft (61 m) (Figure 2). In the coastal exposure, the lower 100 ft (30 m) of this unit consists of mud, peat and sand that backfill a channel cut into sequence T. Overlying the channel deposit is about 100 ft (30 m) of dune sand. Since the sequence's basal channel deposit is probably laterally discontinuous, I assume that unit thickness in most areas approximates the 100 ft (30 m) thickness of the upper eolian unit.

In the Fort Funston well, my pick for sequence U is a clayey sand with a basal elevation of 56 ft (17 m) (Plate E; Appendix B). The electric log for this well begins at a depth of 116 ft (35 m) (Appendix B), so it captures only 50 ft (15 m) of the interval, which is likely thicker. In this location the log shows an upward increase in resistivity, and the driller's log shows a clayey-sand sediment type (Plate E, Appendix B). Using the method described above for sequence S, I tied the coastal exposure to the well.

From Fort Funston, I correlated U to the Zoo MW well by projecting the fold axis using the technique outlined above. My pick for sequence U in the Zoo MW is a 100 ft (30 m) thick package of gray, fine to coarse, poorly to moderately sorted, angular to rounded sand with shells, overlain by a gray mud with organic particles that is overlain by a reddish-brown to grayish-tan, medium to coarse, moderate to well-sorted, sub-angular to rounded sand with some clay (Plate A; Appendix B). The base of this unit is located at an elevation of -485 ft (-148 m). This unit has a negative resistivity kick at its base, followed by an upward increase in resistivity, followed by another negative deflection overlain by a blocky, positive resistivity response that coincides with the upper medium to coarse sand (Plate A; Appendix B).

Moving across the fold from Fort Funston, I correlated sequence U using the method outlined for sequence S. I extended U above T while attempting to maintain unit thickness. I extended U beneath Lake Merced into the LMP well at my target, which is an approximately 50 ft (15 m) thick package at -460 ft (-152 m) elevation (Plate E; Appendix B). The unit consists of mottled gray clay with some sand, shells and organic particles. This unit has a relatively low resistivity that increases slowly upward, and a relatively high gamma response that decreases upward.

Sequence U projects above the top of the Thornton Beach well, so there is no target sequence in the borehole. On the east side of the fold, I again constrained the depth of sequence U using the Rockland ash and the Westlake-2A well. My pick for U in the Westlake well has similar sediment types and log responses to sequence U in the LMP well (Plates D and F; Appendix B). It is an approximately 55 ft (17 m) thick package, located at an elevation of -495 ft (-163 m), consisting of blue clay with shells, and showing a resistivity response that increases slowly upward.

Based on these and other correlations, it appears that from the coastal exposure northward, eastward and southeastward, the dune facies grades laterally into widespread embayment sediments, indicating that an embayment may have formed behind a coastal dune barrier (Figures 4 and 13; Plates A–F).

Sequence V and correlation explanations

Sequence V is exposed at beach level just north of the South Channel (Clifton et al., 1988; Kennedy, 2002). In this area, dips increase northward across the south channel due to the proximity of the fold hinge (Plate 1). Hunter et al. (1984) interpreted V as a progradational sequence approximately 85 ft (26 m) thick (Figure 2). The coastal exposure consists of a basal nearshore sand and gravel overlain by backshore sand, alluvium, and a paleosol cap.

Because of the incomplete well log at the top of the Fort Funston well, it is difficult to determine where and if sequence V intersects the well (Appendix B). Based on my

stratigraphic correlations of lower units and the lack of Colma on the coastal bluff in this location, I show the unit intersecting the borehole at an elevation of approximately 131 ft (40 m) (Plate E; Appendix B).

North of Fort Funston, I correlated sequence V to the Zoo MW well using the method described above. My pick in the Zoo MW well is a 50 ft (15 m) thick package of sandy clay and clayey sand at an elevation of -385 ft (-117 m) (Plate A; Appendix B). This unit has a negative resistivity kick at its base, followed by an upward increase in resistivity.

My pick in the LMP well is an approximately 50 ft (15 m) thick gray, medium-grained, moderate to well-sorted sand with some clay and organic particles (Plate E; Appendix B). The base of this package is located at an elevation of -410 ft (-125 m), and the log response shows consistently high, blocky resistivity values.

Like sequence U, V projects above the Thornton Beach well so it has been eroded away at this location. I extended V on top of U on the eastern side of the fault, again using the Rockland ash and the Westlake-2A well as constraints. I brought V into my Westlake-2A target at an elevation of -337 ft (-142 m) where there is a sand with a blocky resistivity pattern, very similar to V's blocky pattern in the LMP well (Plate E; Appendix B). The log response similarities between the LMP and Westlake–2A wells indicate a continuity of depositional environments (Plate D; Appendix B).

Based on these and other correlations, it appears that the nearshore sediments visible in the coastal bluffs transition to backshore sediments in the zoo area where an embayment may have formed (Plate A). The embayment sediments located in the zoo

area appear to grade eastward into a thick, widespread, sandy unit extending to the south and southeast, that may have been a coastal plain dune field (Plates B–F).

Sequence W and correlation explanations

Sequence W is exposed at beach level approximately 45 ft (115 m) north of the South Channel and it rises in elevation to the south (Plate 1). Hunter et al. (1984) interpreted W as an approximately 55 ft (17 m) thick transgressive sequence, with the lower 25 ft (8 m) being an embayment mud that shallows upward from shelly, channel floor deposits to stratified channel side deposits to bioturbated tidal-flat, sandy mud. This is overlain by about 30 ft (9 m) of sand and gravel interpreted as tidal-inlet deposits (Figure 2).

Sequence W projects above the Fort Funston well so it has been eroded away at this location. I extended sequence W across the fault using the Rockland ash and LMMW-1D and LMP wells as constraints (Appendix C). I extended W over V and brought W through a low resistivity target in the LMMW-1D well at an elevation of -270 ft (82 m) (Plate E). I then pulled W into the LMP well at my 55 ft (17 m) thick, low resistivity target that consists of mottled gray clay mixed with sand and black organic particles (Plate E; Appendix B).

My pick in the Zoo MW well is a 65 ft (20 m) thick package of clayey sand at an elevation of -335 ft (-102 m) (Plate A and Appendix B). This unit shows an upward decrease in resistivity followed by a slightly blocky pattern.

Sequence W projects above the Thornton Beach well, but east of the fold above the concealed Serra fault, I constrained the elevation of W using the Rockland ash and the Westlake-2A well (Appendix C). My target sequence in the Westlake-2A well is a 40 ft (12 m) thick package of mud with a low resistivity log response located at an elevation of -282 ft (-125 m) (Plate F; Appendix B). The log pattern here is again similar to sequence W in the LMP well, indicating a continuity of environments between the two wells (Plate D; Appendix B).

Based on these and other correlations, it appears that north and northeast of the coastal exposure of embayment mud, sequence W appears to grade into sandier sediment (Figures 4, 13 and 14; Plates A–D). During deposition of W, the zoo area may have been a peripheral embayment environment or the embayment may not have extended to this point. To the east and southeast of the coastal exposure, the embayment facies appears to be continuous within the study area.

Sequence X and correlation explanations

Sequence X is exposed at beach level approximately 500 ft (152 m) north of the South Channel and rises in elevation to the south, where it is unconformably overlain by the Colma Formation (Plate 1). Hunter et al. (1984) interpreted X as a complete regressive

sequence approximately 150 ft (46 m) thick, consisting of an inner shelf sand overlain by nearshore, foreshore and eolian sand (Figure 2). Possibly overlying the upper dune facies, but not visible in the cliff face, are "distinctive organic clay and sand beds" that Kennedy (2002) mapped in the intertidal zone, north of the coastal exposure. Hunter et al. (1984) referred to this unit as X5, and described it as consisting of an eolian sand overlain by either a pebbly paleosol or a pebbly transgressive deposit inset into a depression in the upper X4 eolian unit. Kennedy (2002), described the beds as consisting of organic clay and sand, and suggested that they are not visible in the cliff face because they were cut out along an angular unconformity between sequences X and Y. Hunter (2006, pers. comm.) has subsequently concurred with Kennedy's (2002) interpretation. If these organic clay and sand beds represent a fine-grained facies not visible in the cliff face, this unit may be continuous in the subsurface where X and Y are conformable (Plates A–F).

Sequence X projects above the Fort Funston well, but on the east side of the fold above the blind Serra thrust fault, I constrain the unit using the Rockland ash, the LMMW-1D well and the LMP well (Appendix C). My pick for the base of X in the LMMW-1D well is a low resistivity kick at an elevation of -172 ft (-52 m) (Plate E; Appendix B). My pick for sequence X in the LMP well is a 160 ft (49 m) thick gray to reddish-brown, medium, well-sorted sand with traces of wood fragments and shells. This unit has a positive resistivity and a negative gamma ray response, with the blocky look of a thick sandy unit. At an elevation of -220 ft (-67 m) there is a 10 ft (3 m) thick high gamma kick that I correlate as the base of the X5 unit (Plate E; Appendix B).

My pick in the Zoo MW for X is a 130 ft (40 m) thick package, consisting of a sandy clay overlain by a grayish-tan, medium to coarse, moderately-sorted sand with some clay, overlain by a dark gray, medium-grained, very-well-sorted, magnetite-rich sand with shells (Plate A; Appendix B). The electric log for this well shows a sharp, negative resistivity kick at an elevation of -265 ft (-81 m), followed upward by relatively blocky, positive resistivity values, which are punctuated by a low resistivity inflection at an elevation of -195 ft (-59 m). I correlate this uppermost inflection with the X5 unit.

At Thornton Beach, sequence X, like sequences U, V, and W, projects above the well. East of the hinge surface trace of the fold, my pick in the Westlake-2A well is a 130 ft (40 m) thick package of fine sand with some clay (Plate F; Appendix B). This lithologic unit has a notably blocky, positive resistivity pattern very similar to the pattern in the LMP well, again suggesting a continuity of depositional environments between the wells (Plate D).

Based on these and other correlations not mentioned here, to the north, it appears that the inner-shelf /nearshore sediments of the coastal exposure grade into backshore sediments and that an embayment may have formed behind a coastal barrier (Figures 4, 13, 14; Plate A). This embayment at the base of X appears to have existed in the zoo area and extended in a narrow band to the southeast (Figures 13 and 14). A thick accumulation of sand in both the LMP and Westlake-2A wells at similar elevations suggests that the embayment may have extended between these locations (Plates B,–F; Appendix B). A second embayment, possibly Hunter et al.'s (1984) X5 unit, may

extend north, northeast, east and southeast in the subsurface from the beach. Near the LMP well, however, X5 grades into coarser sands, and the embayment facies appears to be somewhat discontinuous (Plates B, C and E).

Sequence Y and correlation explanations

Sequence Y is exposed at beach level approximately 1100 ft (340 m) north of the South Channel (Plate 1) and rises in elevation to the south where it is unconformably overlain by the Colma Formation. The unit extends northward along the beach. The contact between Y and the underlying sequence X has been interpreted as an angular unconformity by Kennedy (2002), as described above. Hunter et al. (1984) interpreted sequence Y as an approximately 50 ft (15 m) thick, progradational sequence (Figure 2). The coastal exposure consists of nearshore sand and gravel overlain by foreshore and backshore sand. Hunter et al. (1984) noted that the nearshore and foreshore gravel and sand of this unit are uniquely characterized by the presence of mica, suggesting a proximal source of suspended sediment.

Sequence Y, like X and W, projects above the Fort Funston well. My pick in the LMMW-1D well is a 60 ft (18 m) thick package of brown, fine to medium sand with a relatively positive resistivity that increases upward (Plate E; Appendix B). The base of this unit is located at an elevation of -92 ft (-28 m). My pick in the LMP well is a 70 ft (21 m) thick package of gray, fine to medium, very-well-sorted sand overlain by a

gray, fine to medium, well-sorted sand with shells and organic particles located at an elevation of -125 ft (-38 m) (Plate E; Appendix B).

My pick in the Zoo MW for Sequence Y is a 60 ft (18 m) thick package of gray, sticky, mud with shells overlain by very well-rounded gravel with some sand and abundant shells (Plate A; Appendix B). This package has a notably low resistivity response and is located at an elevation of -135 ft (-41 m).

Sequence Y is not present in the Thornton Beach well, but east of the hinge surface trace of the fold above the concealed Serra fault, I constrained the sequence boundaries using the methods described above. My pick for sequence Y in the Westlake-2A well is a 80 ft (24 m) thick package of clay and sandy clay located at an elevation of -122 ft (-37 m) (Plate F; Appendix B). This unit has a negative resistivity kick at a basal elevation of -122 ft (-37 m), followed by an upward increase in resistivity, followed by another negative deflection that decreases upward.

Based on these and other correlations not described here, it appears that to the north and northeast, the nearshore sediments of the coastal exposure transition into backshore sand and fine-grained embayment sediment (Figures 4, 14 and 15; Plates A, E and D). Based on my model, a northwest-trending embayment appears to have formed behind a northwest-trending coastal barrier (Figure 15). The embayment sediments appear to interfinger with alluvium to the east and southeast, whereas coarse sand and gravelly clay in the zoo area indicate this may have been a tidal channel or embayment inlet during deposition of this sequence (Figure 4; Plates B–F).

Colma Formation (sequence Z) and correlation explanations

An approximately 1-m-thick erosional remnant of the Colma Formation lies in angular discordance on sequences V, X and Y north of Fort Funston (Plate 1; Clifton et al., 1988; Yi, 2005). Yi (2005) noted that the Colma in this location contains heavy mineral laminations and is most likely a foreshore or backshore deposit. To the south, near Thornton Beach, where the Colma unconformably overlies sequence S of the Merced Formation, Yi (2005) measured an 11-13 m thick section of Colma sediment that consists of nearshore, foreshore, backshore and dune deposits (Plate 1).

I assume there is little to no Colma Formation located at the top of the Fort Funston well, based on surface mapping (Bonilla, 1971; Kennedy, 2002), and the absence of visible Colma in the coastal bluffs 800 ft (240 m) west of the well. East of the surface trace of the fold hinge, I constrain the location of the Colma using surface mapping (Bonilla, 1971; Kennedy, 2002) and the methods described above, while accounting for angular discordance near the fold trace. My Colma pick in the LMMW-1D well is a large, positive resistivity kick at an elevation of -22 ft (-7 m) (Plate E). The sediment package consists of brown, very fine to medium grained, sub-rounded to rounded sand with some silt and organic particles. It is not clear how thick the Colma is at the location of the LMMW-1D well. Holocene sand is mapped in this area (Bonilla, 1971; Kennedy, 2002), and from the top of the well to the base of my Colma boundary is about 70 ft (21 m). The Colma, as I have delineated it, is approximately 50 ft (15 m) thick, which seems possible, given that in the Harding Park Golf Course,

approximately 2600 ft (800 m) to the northeast, the Colma is as thick as 75 ft (23 m) (Bonilla, 1971; Kennedy, 2002).

Approximately 100 ft. (30 m) of Colma sediment is mapped near the LMP well (Bonilla, 1971; Kennedy, 2002). My pick in the LMP well is a reddish-brown, fine to medium, very-well-rounded and well-sorted sand, with a basal elevation of -60 ft (-18 m), or about 100 ft (30 m) below the top of the well (Plate E; Appendix B). The base of my Colma target here shows an upward increase in resistivity.

My pick for the Colma sequence in the Zoo MW well is an approximately 100 ft (30 m) thick, very coarse, well-sorted and well-rounded sand, that has a positive resistivity kick at an elevation of -75 ft (-22 m) (Plate A; Appendix B). This sand is overlain by a lower resistivity, gray to black, medium, very-well-sorted sand with magnetite and shell fragments. This sand is overlain by a 30 ft (9 m) thick reddish-brown, fine to coarse, moderately-sorted sand.

At Thornton Beach, Yi (2005) measured an approximately 38-39 ft (11–13 m) thick section of Colma deposits unconformably overlying sequence S of the Merced Formation. Using this stratigraphic relationship, my pick for the Colma in the Thornton Beach well is the contact above sequence S at an elevation of -160 ft (-49 m) (Plate F, Appendix B). At this elevation, there is a positive resistivity kick, coinciding with 15 ft (5 m) thick, tan, medium to coarse, well-sorted sand with some clay. Above this sand is a dark, gray to black, fine to medium, well-sorted sand with magnetite.

Based on surface mapping (Bonilla, 1971; Kennedy, 2002) the Colma is not present along cross section F-F' in the "break of slope" location where I have labeled a possible fold hinge trace (Plate F). However, the Colma crops out down slope and I therefore project it to the Westlake-2A well while accounting for angular discordance near the fold trace. My Colma pick in the Westlake well is an approximately 100 ft (30 m) thick, high resistivity zone with a basal elevation of -42 ft (-13 m) (Plate F; Appendix B). This sandy package is overlain by a 70 ft (21 m) thick, low resistivity, sandy clay, which may or may not be part of the Colma.

Based on these and other correlations, it appears that the Colma sequence thins along the coast above the Serra blind thrust, but thickens to the north, northeast, east and southeast (Plates A–F). The coastal exposures have been interpreted by Yi (2005) to be primarily nearshore, foreshore and backshore deposits. Based on the excellent sorting and lack of shells in sand to the east, it appears that most of the Colma within the study area may have been backshore dunes that interfinger with alluvium east and southeast of Lake Merced (Plates B–F). From where the Colma interfingers with the alluvium, it appears to form a terrace-like surface that slopes towards the ocean. This surface was likely incised during the last sea level low stand and the incised valleys were partially filled during the subsequent (Holocene) transgression, forming Lake Merced.

Correlations of sequences R-N from coastal exposures to the Fort Funston, Thornton Beach and Zoo MW wells

In my stratigraphic analysis, I do not describe in detail the sequences below S (sequences N-R) shown on cross sections A-A', E-E, and F-F' (Plates A, E and F). I focused on the units above sequence R because they appear to be the primary aquifer-forming strata that extend beneath Lake Merced. However, based on my model, sequences Q and R may have subsurface aquifer-forming strata between the western edge of Lake Merced and east of the fold axis, as mapped by Kennedy (2002) (Plates E and F). In this section, I describe sequence R, because it crops out at beach level near Fort Funston, and its identification substantiates my sequence S correlations, which form the foundation for all subsequent correlations.

Sequence R is exposed at beach level directly west of the Fort Funston well (Plate 1). The unit rises in elevation to the south where it is disrupted by the landslide complex between Fort Funston and Thornton Beach. Hunter et al. (1984) described R as an approximately 200 ft (63 m) thick regressive sequence, consisting of a thick, 115 ft (35 m) basal embayment mud overlain by 60 ft (18 m) of dune sand, which is overlain by almost 33 ft (10 m) backshore sand, paleosols and alluvial deposits (Figure 2). The lower embayment mud consists of laminated muds overlain by fining-upward tidal-channel sequences with shell lags (Hunter et al., 1984).

To correlate sequences N–R from coastal exposures to the Fort Funston and Thornton Beach wells, I used the same technique that I used for correlating upper units (S–Z) to the coastal wells. My pick for sequence R in the Fort Funston well is an approximately 220 ft (67 m) thick unit consisting of a basal 50 ft (15 m) thick, dark sandy-clay to clay with shells, overlain by a 100 ft (30 m) package of greenish-gray, sandy-silt with shells, overlain by a 70 ft (21 m) thick greenish gray, sandy-silt without shells (Plate E; Appendix B). This unit is marked by a well-defined, low resistivity zone at an elevation of -254 ft (-77 m). This low resistivity zone kicks in the positive direction at an elevation of -214 ft (-65 m), and maintains a relatively uniform resistivity upward (Plate E; Appendix B).

Using the method outlined above, I projected the fold axis mapped by Kennedy (2002) inland to the line of cross section A-A', and brought units R–N across the fold to depth where they lapped onto the bedrock surface before reaching the Zoo MW well (Plate A).

In the Thornton Beach well, my pick for R is an approximately 230 ft (70 m) thick package of clay and sand with shells overlain by a reddish-brown, medium to coarse, well sorted, sub-rounded to rounded sand (Plate F; Appendix B). The base of R in this location is marked by a negative resistivity inflection that coincides with a 70 ft (21 m) thick gray mud with traces of sand and shells at an elevation of -90 ft (-27 m). The resistivity increases upward through this interval but deflects in the negative direction

at the contact with a clayey sand with shells. Above this, the unit's resistivity abruptly becomes more positive within the reddish-brown sand unit (Plate F; Appendix B).

Based on these correlations it appears that the embayment sequence that is exposed in the outcrop below Fort Funston extends to the Fort Funston and Thornton Beach wells. The basal mud varies in thickness from the coastal exposure to the wells, but this can be explained by localized tidal channels or other lateral facies changes within the embayment system. The overall package of the infilling of an embayment is seen in both the coastal exposures and the wells.

After substantiating my sequence S correlation with the R correlation, I extended the stratigraphic section downward for sequences Q-N, using the same technique, while attempting to maintain unit thickness, and correlating sediment type and electric log response between the coast and the wells.

Depositional Environments and Paleogeographic Model

After correlating sequences between coastal outcrops and inland wells, and producing six cross sections, I developed a paleogeographic model of the coastal region during the past ~500 ka (depositional period of sequences S–Z) (Figure 4). I propose that sequences S through Z were deposited in beach/barrier/embayment environments during successive sea-level high stands associated with global interglacial cycles (Clifton et al., 1988). Because there appear to be backshore rather than nearshore

sediments in the three coast-adjacent wells north of the zoo area (Taraval MW, Ortega MW, Kirkham MW), I hypothesize that the paleo-coastlines trended more northwesterly than the present shoreline and were oriented roughly parallel to the northwest–southeast trending bedrock escarpment beneath the Lake Merced area (Figures 4 and 12). Behind these shorelines and their associated barrier dunes, a succession of northwest–southeast trending embayments formed during sea-level high stands (Figures 13, 14 and 15). The fine-grained sediments deposited in these embayments now form a series of vertically separated aquitards. Low-stand components of sea-level cycles are expressed primarily as erosion surfaces that form unconformities between the vertically-stacked sequences.

A variety of sediment types were deposited within these paleo-embayment systems (Figure 4). Clayey, well-sorted gravel with shells, found at various depths in the San Francisco Zoo area, indicates that this location may have been an embayment inlet or tidal channel during the deposition of several high-stand sequences. Mud and organic mud found at various depths in the LMP well indicate that this area may have been a peripheral salt marsh and tidal flat or a central, low-energy environment during the deposition of several embayments (Figure 4; Plates B–E; Appendix B).

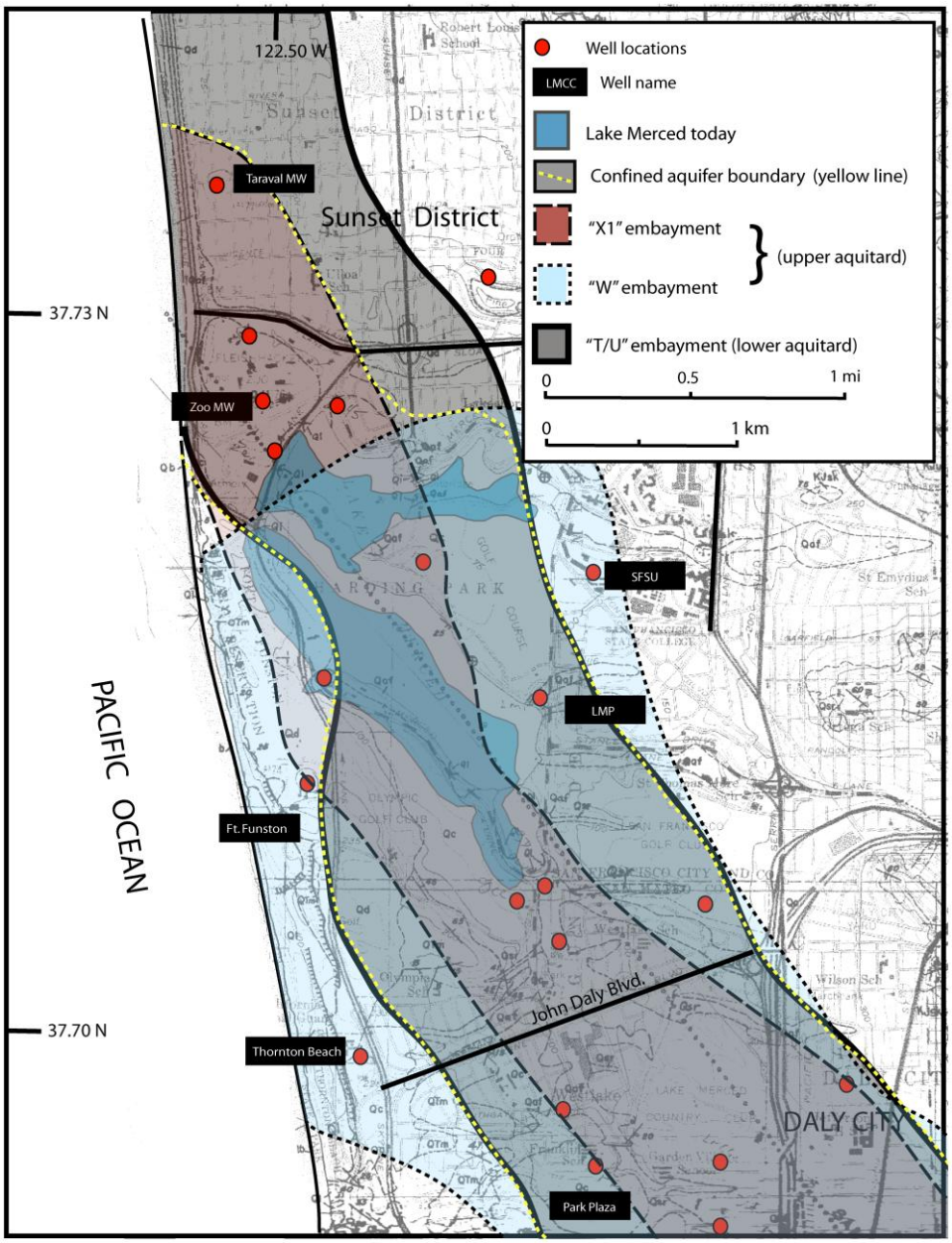

Figure 13. Paleogeographic map showing the inferred boundaries of the "T/U", "W" and "X" embayments, which form the lower and upper confining units for *Aquifer V*. Base map from Bonilla (1971).

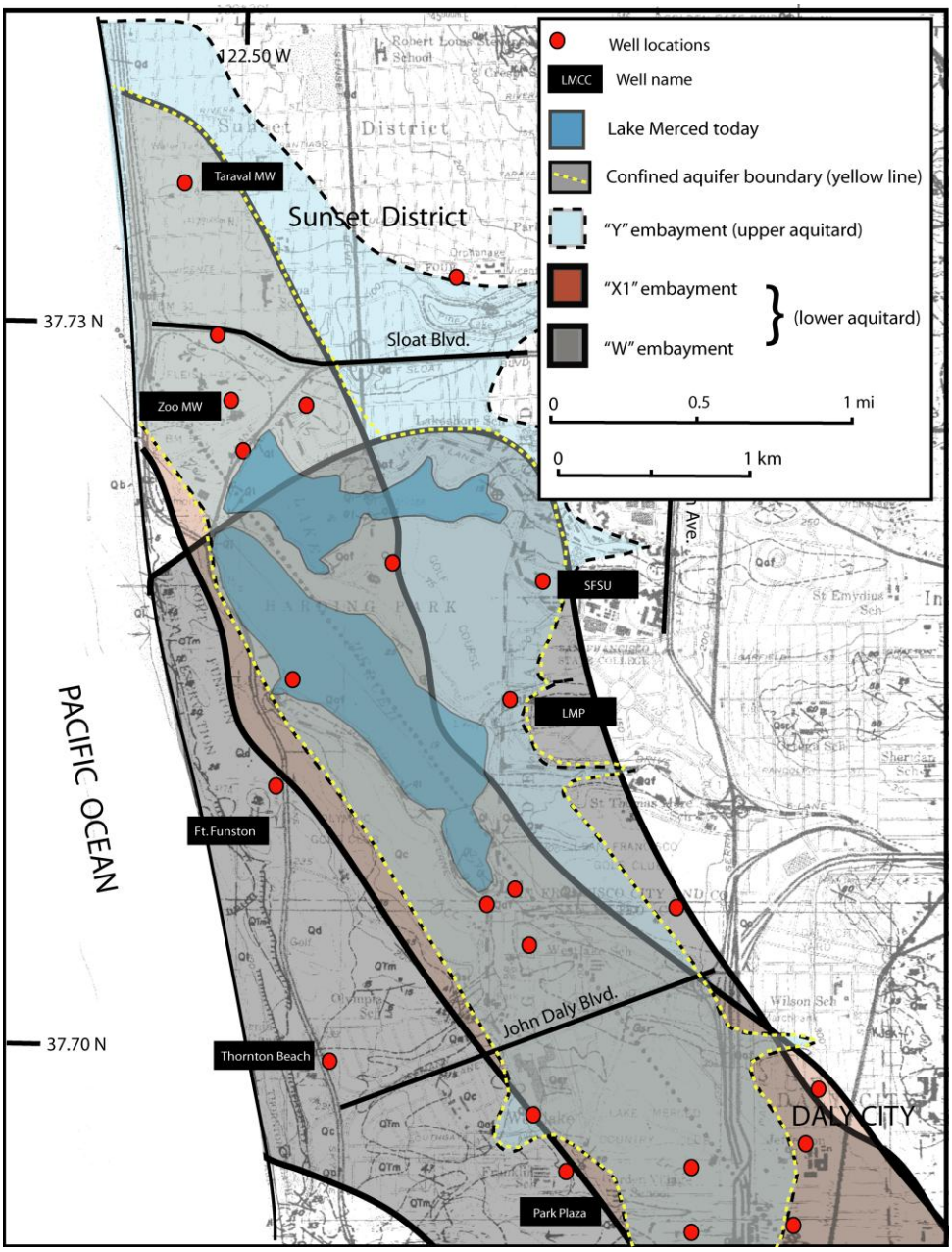

Figure 14. Paleogeographic map showing the inferred boundaries of the "W","X" and "Y" embayments, which form the lower and upper confining units for *Aquifer X*. Base map from Bonilla (1971).

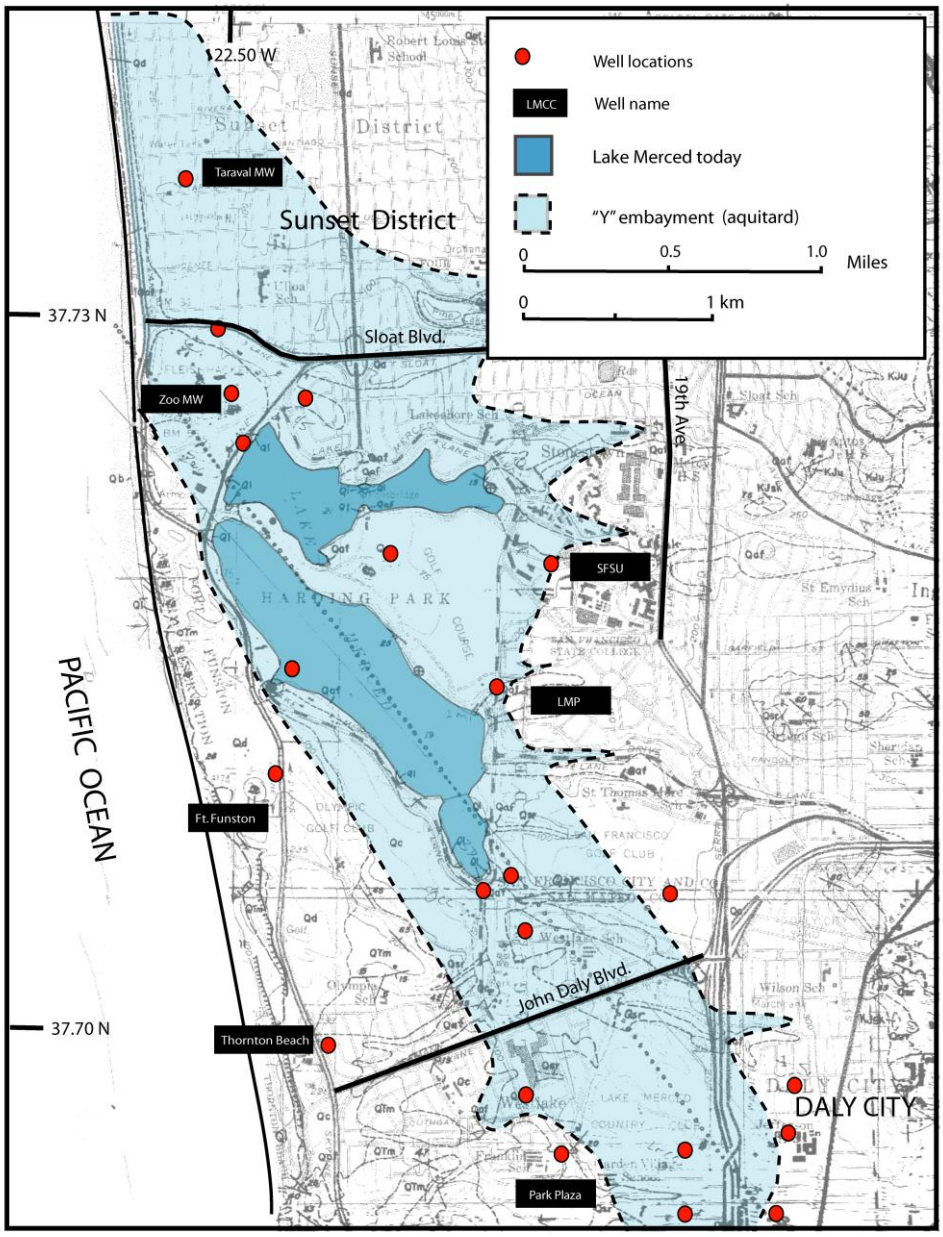

Figure 15. Paleogeographic map showing the inferred boundary of the "Y" embayment, which forms the aquitard for the unconfined *Aquifer Z*. Base map from Bonilla (1971).

North and northeast of Lake Merced, mud and silty sand transition to more sandy strata, indicating that the areas north of the lake may have been a persistent backshore dune field (Figure 4; Plate A; Appendix A). From these dune fields and coastal barriers, sand was likely blown into embayments, creating silty-sand and sandy-mud deposits around the edges of these bays (Figure 4).

East and southeast of Lake Merced, oxidized, clayey sand and gravel interfinger with silty-sand and mud, indicating that alluvium prograded from highlands into the embayments (Figure 4; Plates B, C, E, and F; Appendix A). Coarser, less-rounded, more poorly-sorted sand and gravel found in various well locations indicate that alluvial material was carried into embayments from local creek channels draining the highlands.

Aquifers and Aquitards

The sedimentary units in the North Westside Basin appear to form three layered aquifers. From the surface downward I have labeled them the "Z" (Colma), "X" and "V" aquifers (Figures 13, 14 and 15; Plates A-F). In the groundwater basin, the aquifers are formed in sandy sediment deposited in backshore environments. The aquitards are formed by muddy sediment deposited in paleo-estuarine environments (Figure 4).

Aquifer Z is unconfined and bounded at the base by paleo-embayment sediments associated with sequence Y (Figure 15, Plates A–F). Lake Merced is nested in this aquifer, which appears to be 50 to 100 feet (15–30 m) thick, with an area approximating the size of the aquitard formed by the paleo-embayment sediments of sequence Y (Figure 15). Vertical flow in the aquifer likely becomes less restricted north and northeast of Lake Merced, where the paleo-embayment facies of sequence Y transitions to more permeable dune facies (Figure 15; Plate A). Lateral flow is likely restricted southwest of Lake Merced due to folding of fine-grained sediments along the Serra blind thrust fault, and deformation on the eastern part of the basin may also restrict flow (Figures 5 and 15; Plates E and F).

Aquifer X is relatively confined and appears to be the largest of the three aquifers. The unit is bounded at the base by paleo-embayment sediments of sequences X and W and confined at the top by the paleo-embayment sediments of sequence Y (Figure 14). Based on our model, the aquifer is 100–150 feet thick within the study area, and its area in this part of the basin approximates the *overlapped portions* of the upper and lower confining units (Figure 14). This aquifer can be divided into an upper and lower unit by sediments of paleo-embayment X5; however, this unit appears to be discontinuous around LMP and would allow vertical communication between the upper and lower units (Plates B, C and E). Lateral flow is likely restricted southwest of Lake Merced by folding along the Serra blind thrust fault and lateral flow may be restricted to the northeast and east where confining layers of Y and W are uplifted (Figure 5; Plates E, F and D).

Aquifer V is relatively confined, bounded at the base by paleo-embayment facies of sequences T and U and capped by paleo-embayment facies of W and X (Figure 13; Plates A-F). Based on our model, the aquifer appears to be about 60 ft (18 m) thick, but may thicken to the north and northeast where upper confining sediments of sequence W transition to coarser, sandy material and sequence X caps the unit (Figure 13; Plate A). In this area, the aquifer may be as thick as 160 ft (49 m). Aquifer V's area in this part of the basin approximates the *overlapped parts* of the upper and lower confining units (Figure 13); lateral flow is likely restricted southwest of Lake Merced by deformed fine-grained strata above the Serra blind thrust fault and to the northeast and east of the lake due to faulting or folding (Figure 5; Plates D–F).

Comparison with water quality analysis

After completing my analyses, I compared my results to Wood's (2008) analysis of water-quality data acquired from some of the same wells used in my study. As described in the previous section, I propose that fine-grained sediments, deposited in embayment environments during several sea level highstands, now form aquitards in the North Westside Basin. Using plates A–F, I mapped the approximate boundaries of these embayments and show them in Figures 13, 14 and 15. Wood (2008) compiled and statistically analyzed existing water-quality data in the basin in an effort to delineate hydrostratigraphic units. Operating under the assumption that water drawn from discreet subsurface intervals represents the water quality of the adjacent aquifer, Wood (2008) used Piper and Stiff quantitative analyses of ion concentrations, along

with temporal and spatial analyses (TSAN) of water quality parameters, to locate the depths and extents of apparent barriers to subsurface flow. An important first step in Wood's (2008) research was deciding which data would be most useful. The data that provided the best opportunity to study water quality came from the coast-adjacent wells located west and northwest of Lake Merced (Figure 16; Zoo MW, Zoo #5, Taraval, Ortega and Kirkham). These locations were best suited because each consists of a nested well complex where several distinct wells were drilled and screened at separate depths to allow the collection of unmixed samples from separate aquifers. Wood's (2008) analysis of water-quality data from the coast-adjacent wells are consistent with my stratigraphic analysis. The three deepest wells at the Zoo MW, Taraval and Ortega locations show similar water quality to each other, but different water quality from all overlying nested wells. This indicates that the three deepest wells are hydrologically connected to each other but separated from the wells above by a less-permeable unit, which coincides with the sediments associated with the T/U embayment (Figures 13 and 16; Plate A). At a higher level, Wood (2008) found a difference between the water of the two middle Taraval wells. This indicates the presence of a less-permeable layer that coincides with the depth of embayment sediments associated with sequence X (Figures 14 and 16, Plate A). A temporal and spatial analysis (TSAN) of these data also concurs with my stratigraphic interpretation

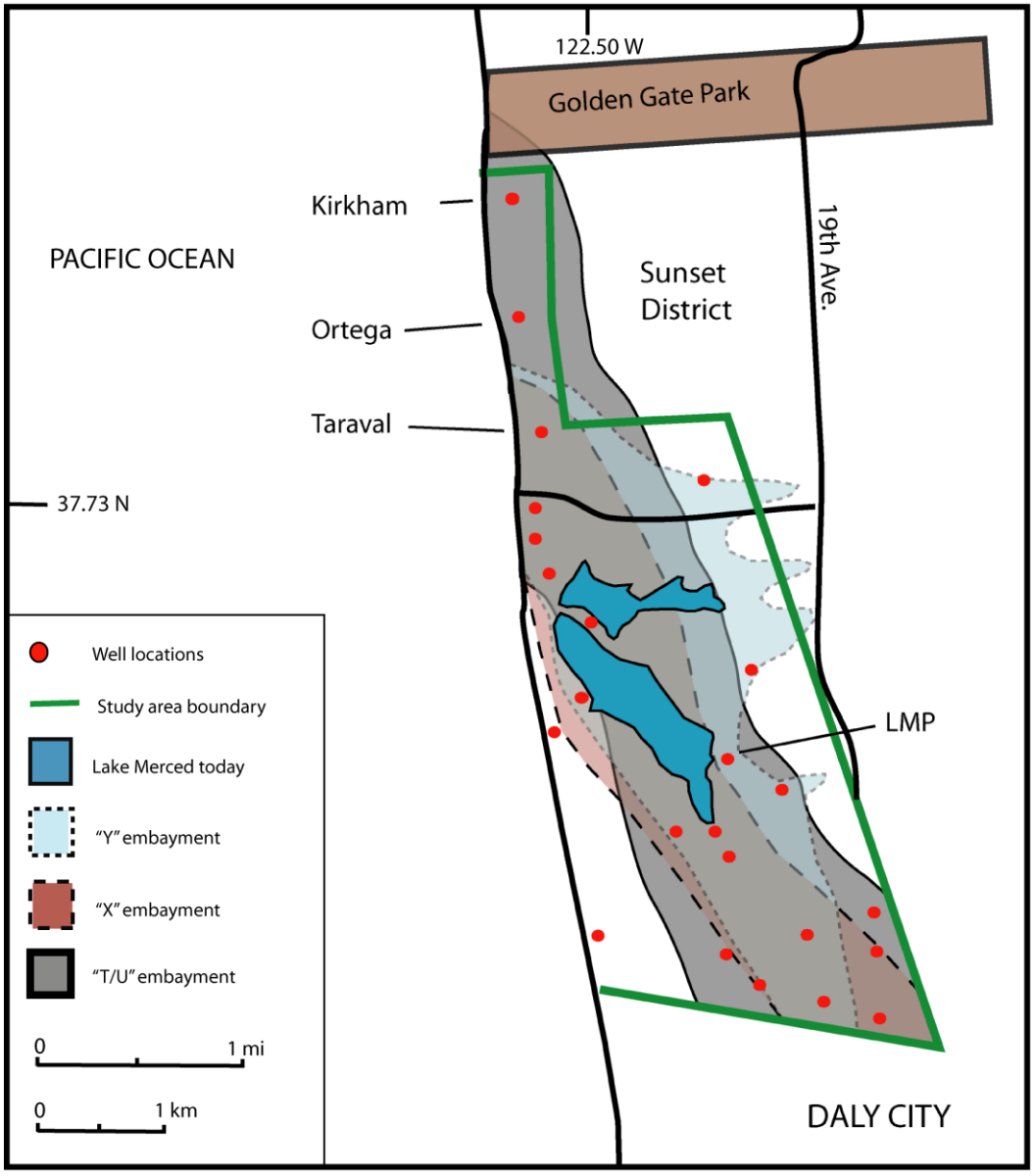

Figure 16. Location of coast-adjacent wells (Kirkham, Ortega and Taraval) used by Wood (2008). Figure also shows predicted paleoembayment boundaries in relation to the wells used in Wood's (2008) study.

and suggests that this less-permeable layer pinches out between Taraval and Ortega (Plate A). There was also a water quality difference between the upper two wells at Taraval, suggesting a less-permeable unit between the two wells that coincides with the embayment sediments of Sequence Y (Figures 15 and 16; Plate A). The TSAN of

these data, however, suggest that this unit extends beyond Ortega, pinching out before reaching the northernmost Kirkham well. Finally, Wood (2008) found that all wells in the Kirkham complex have similar water quality to each other, but different water quality than all other coastal wells. This is also in agreement with my stratigraphic interpretation that all of the less-permeable embayment units above sequence T pinch out south of Kirkham, and that the sediments at Kirkham are sandy (i.e., more permeable) throughout (Figure 16; Plate A). Because the coastline trended more to the northwest than the current coastline (Figure 4), the area around Kirkham was continually located in a non-marine, sandy environment, landward of the embayments that were formed along the coast farther south.

Wood (2008) also analyzed water-quality data from the wells south of Lake Merced. Data from these wells showed less clear trends and were often collected from long screened intervals that made it difficult to know from which depths the data were collected. In general, Wood (2008) found that the less-permeable units were not as continuous south of the lake, consistent with my interpretation that some of the sediments in these wells were deposited in an alluvial environment where the less-permeable (i.e., clay-rich) units are less common and less continuous than they are in the embayment environments to the north (Figure 4; Plates B, C, E and F).

Pleistocene sea level fluctuations related to Merced sequences

Sediment preservation in any basin depends of the amount of vertical space below base level that is available to accumulate sediments, a volume referred to as "accommodation space" in the terminology of sequence stratigraphy. In marginal marine basins, where base level is the level of the sea, accommodation space is controlled by eustatic sea-level change, vertical motion of the basin floor and sedimentation rate. Clifton et al. (1988) and Ingram and Ingle (1998) investigated the relationship between Merced Formation sequences and Pleistocene eustatic sea-level fluctuations. Using Shackleton and Opdyke's (1976) $^{18}O/^{16}O$ ratios and the Merced age data available at that time, Clifton et al. (1988) calculated the approximate sea-level changes suggested by the $^{18}O/^{16}O$ ratios and compared this curve to a Merced Formation, sedimentology-based, paleo-bathymetry curve. They found that the two curves are difficult to match, possibly due to: the inaccuracy of the sea level curve, loss of section (i.e., erosion) in the Merced, unrecognized water-depth changes in shelf facies that represent small scale sea-level fluctuations and/or other tectonic or sedimentologic effects (Clifton et al., 1988**).** Ingram and Ingle (1998), using strontium isotope dating of sequences, concluded that sequences deposited between 600 ka (approximately sequence P) and the present have a cyclicity of approximately 100,000 yr and appear to be controlled by Pleistocene sea-level fluctuations. Using Ingram and Ingle's (1998) youngest three data points (located in sequences O, I and F) and age data for the Rockland ash and Colma Formation, I further examined how sequences F–Z

can be fit to the latest OIS curve (Lisiecki and Raymo, 2005), to investigate the controls of eustasy and localized tectonic subsidence on sequence formation.

After plotting the Merced age ranges on the OIS curve (Figure 17), I created Models A and B (Figures 18 and 19) in which I examined the sequence intervals F-O, O-S and S-Z. Sequence F has an age range of 700–800 ka and sequence O has an age range of 590–650 ka (Figure 17; Ingram and Ingle, 1998). Using the oldest age for sequence F and the youngest for sequence O, provides approximately 210,000 yr for the deposition of 1200 ft (375 m) of section containing 9 unconformities (Figure 18; Clifton and Hunter, 1987). The calculated subsidence rate for this interval is 1.8 mm/yr. It is not possible to match individual transgressions with individual high stands in this time interval and, if the dates are correct, it appears that multiple sequences formed during highstands, or that sequences may also have formed during low stands (Figure 18). This result suggests a strong tectonic control, in addition to the eustatic sea level control.

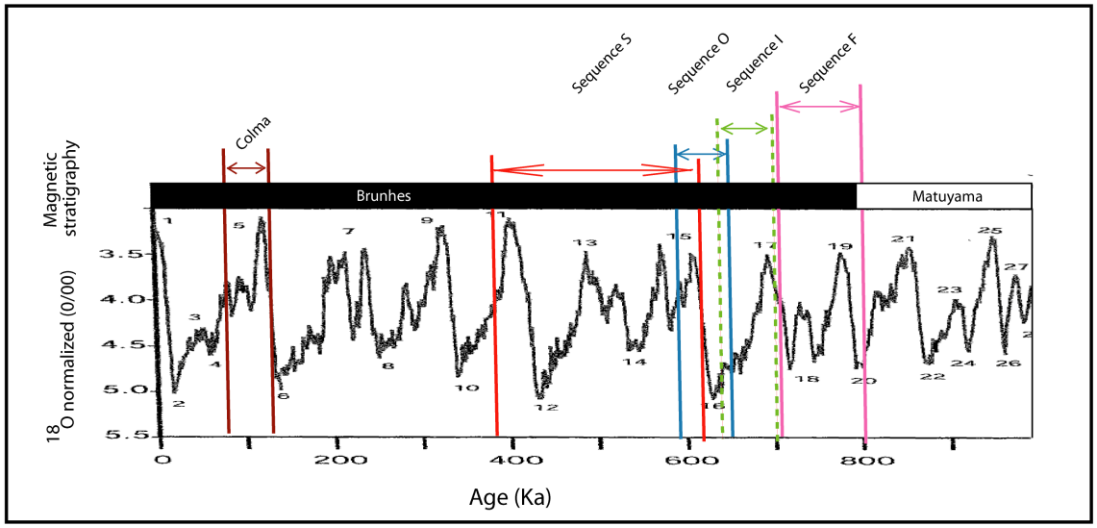

Figure 17. Pleistocene oxygen isotope stage (OIS) curve of Lisiecki and Raymo (2005), with Merced Formation age ranges. See Table 1 for sources of age data.

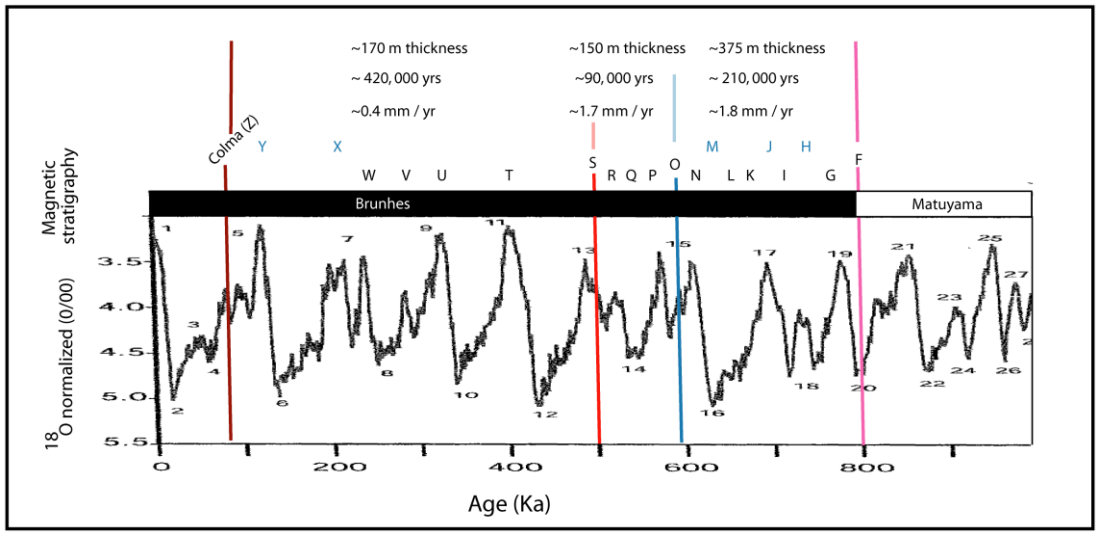

Figure 18. Model A. Pleistocene OIS curve of Lisiecki and Raymo (2005), with Merced Formation sequence designations (letters F–Z), interval thicknesses, estimated depositional times and subsidence rates. Model A uses a 500 ka age estimate for the Rockland ash (sequence S). Blue letters indicate sequences with bounding unconformities that separate depositional environments with relatively greater water depth changes; these sequences are most likely to correlate with OIS high-stand peaks.

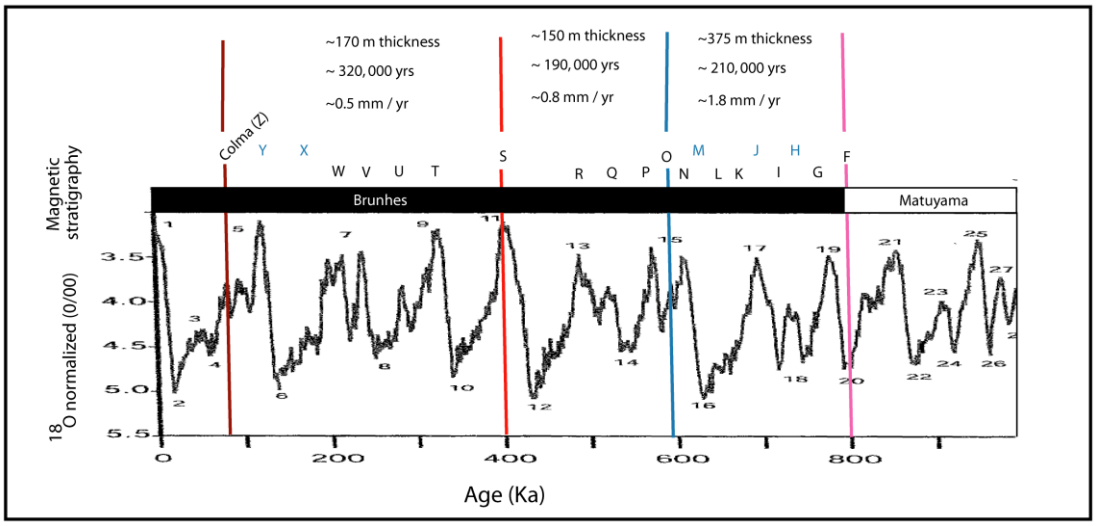

Figure 19. Model B. Pleistocene OIS curve of Lisiecki and Raymo (2005), with Merced Formation sequence designations (letters F–Z), interval thicknesses, estimated depositional times and subsidence rates. Model B uses older age estimate for Rockland ash (sequence S). As in Figure 18, blue letters indicate sequences most likely to correlate with high-stand peaks on the curve.

In considering a strong tectonic signal, it is helpful to conceptualize the elevation difference and lateral separation of local modern depositional environments (as a model for the past) in order to estimate the relative sea level change required for the formation of a sequence boundary. Using Lake Merced as a "paleo-embayment" location (elevation ~6 m), and the modern day beach as the foreshore (elevation 0 m), the distance separating these environments varies from 500 m to about 1.5 km. Assuming that nearshore deposits now exposed on the coastal bluff represent the approximate location of several paleo-shorelines, and considering the distance and elevation change between environments, it seems likely that a 20 ft (6 m) relative increase in sea level (combination of subsidence and eustatic rise), could force a transgression, and subsequent lateral translation of nearshore sand and gravel over backshore embayments, or shelf over nearshore environments. It seems possible that

within the sequence F–O interval, the Merced basin may have been "sensitive" to small sea level fluctuations not evident in the OIS curve. Small peaks within individual high stands may represent relatively small (possibly 20 ft / 6 m) sea-level fluctuations that, coupled with higher tectonically-driven subsidence rates, caused transgressions.

Examining the sequence O-S interval, with a sequence O age of 590 ka and a sequence S age of 500 ka (Model A-based on a Rockland ash age midway between the minimum and maximum estimates), provides 90,000 yr for the deposition of approximately 500 ft (150 m) of section containing 4 unconformities (Figure 18; Clifton et al., 1988). The calculated subsidence rate for this interval is 1.7 mm/yr. Within this interval it is not possible to assign individual sequences to individual highstands; however, an alternate model with a younger age for sequence S (Model B-based on a 400 ka age estimate for the Rockland ash), provides 190,000 yr for the deposition of this interval, yielding a subsidence rate of 0.8 mm/ yr, and a better fit to the OIS curve (Figure 19).

Based on models A and B, the interval between sequence S and the Colma Formation (Models A and B assume an approximately 80 ka age for the Colma) provides from 320,000 to 420,000 yr for the deposition of approximately 550 ft (170 m) of section that comprises 7 unconformities, the upper two of which are angular unconformities (Figures 18 and 19). The calculated subsidence rate for this interval is from 0.4 to 0.5 mm/yr. In this interval it is easier to match individual sequences to peaks on the OIS curve. This suggests, as Ingram and Ingle (1998) noted, that transgressions above approximately sequence P appear to be more correlative with highstands. This idea is

also supported by Hall's (1965) observation of a provenance change within sequence P, which is thought to signal the opening of the Sacramento-San Joaquin drainage through the Golden Gate. If this drainage change increased the sedimentation rate, causing progradation, and the sedimentologic shift from primarily offshore (shelf) deposition below P to terrestrial (backshore) deposition above (Clifton et al., 1988), it follows that greater relative changes in sea level would be needed to force transgressions. Clifton et al., (1988) also note this, stating that the nearshore deposits that formed above sequence P likely formed during high stands. Therefore, eustatic change appears to be the primary transgression driver in sequences above P, whereas between sequences F and O, transgressions appear to be primarily tectonically driven.

CONCLUSION

The Merced and Colma Formations are uplifted and exposed in the coastal bluffs southwest of San Francisco. These units, which extend to the southwest in a narrow outcrop band, are the primary geologic units in the North Westside Groundwater Basin. The goal of my study was to correlate coastal outcrops of the Merced and Colma Formations to inland wells, using geophysical data, well cuttings, drillers' logs, sequence facies and thickness data, bedrock surface geometry, global sea level and structural data. Using these data I created a subsurface model depicting the location of aquifers and aquitards within the North Westside Groundwater basin in the areas surrounding Lake Merced. I also generated generalized and specific paleogeographic/depositional models, compared my stratigraphic data to recent ground

water data and examined the relationship between Pleistocene sea level change and Merced sequence formation.

My stratigraphic model indicates that Merced/Colma sequences S through Z are the primary aquifer forming strata in this part of the basin and sequences T, X and Y which contain high-energy, nearshore facies in the uplifted coastal bluff exposures (Clifton et al., 1988), transition inland to low-energy embayment facies. This, coupled with the presence of other embayment-dominated sequences visible in the coastal bluffs, indicates that sequences S-Z were deposited in a beach-barrier-embayment system that, based on sedimentologic data, appears to have had a paleoshoreline that trended more to the northwest than the present-day shoreline. Behind this paleo-shoreline, northwest–southeast-trending emabayments produced fine-grained sediments that now form a series of aquitards in the subsurface. These aquitards divide the strata beneath Lake Merced into three aquifers. Lake Merced is nested in the upper, unconfined aquifer I call aquifer Z. Aquifer X is contained within sequence X and is relatively confined; Aquifer V is also relatively confined and contained within sequence V.

The Merced and Colma strata that comprise these aquifers are uplifted as much as 800 ft (240 m) southwest of Lake Merced, where a fault-propagation fold above the concealed Serra thrust fault has produced a northeast-vergent monoclinal fold (Kennedy, 2002). Trending sub-parallel to the hinge-surface trace of the fold above the Serra fault, in the eastern part of the study area, there appears to be deformation that uplifts strata, but much less than does the fold above the concealed Serra fault. The

fold above the Serra fault, and deformation in the eastern part of the study area, fold aquifer-forming strata into a broad northwest–southeast-trending, asymmetric syncline whose limbs open and flatten to the northwest. The stratigraphy and structure appear to form a northwest–southeast-trending, compartmentalized, bowl-shaped aquifer that becomes less laterally restricted and more vertically homogenous to the north and northeast within the study area.

The stratigraphic model I propose is in agreement with a recent water-quality study of coast-adjacent wells (Wood, 2008). Using a series of nested well complexes extending from Kirkham Avenue, southward to the San Francisco Zoo, Wood's (2008) goal was to delineate hydrostratigraphic units by statistically investigating water-quality differences at various depths. Wood's (2008) analyses indicate the presence of several aquitards that correlate closely with several embayment facies I have predicted in my stratigraphic model for this coast-adjacent area north of the San Francisco Zoo.

Finally, building on the work of Clifton et al. (1988) and Ingram and Ingle (1998), I examined the relationship between Merced sequence formation and Pleistocene eustatic sea level fluctuations. Using Clifton et al.'s (1988) coastal stratigraphy, along with existing Merced and Colma age data, I attempted to match Merced sequence boundaries F through Z to sea level high stands indicated by the most recent OIS curve of Lisiecki and Raymo (2005). In the stratigraphic section above sequence P, it is relatively easy to match peaks on the OIS carve to Merced sequence boundaries, whereas below sequence P, there are more sequence boundaries than there are sea-level high stands. This may indicate that between sequences F and P, the Merced basin was

more “sensitive” to small sea-level fluctuations not evident in the OIS curve, and that transgressions were primarily tectonically driven whereas above P they were likely eustatically driven.

REFERENCES

Atwater, T., and Stock, J., 1998, Pacific-North America plate tectonics of the Neogene Southwestern United States; An update: International Geology Review, v. 40, p. 375-402.

Barr, J., 1999, Northern continuation of the Serra fault to southwest San Francisco: constraints on uplift rates and style of deformation on the San Francisco Peninsula: unpublished undergraduate thesis, San Francisco State University, 21 p.

Bonilla, M.G., 1971, Preliminary geologic map of the San Francisco South Quadrangle and part of the Hunter's Point Quadrangle, California: U.S. Geological Survey Miscellaneous Field Studies Map MF-311, scale 1:24,000.

Brabb, E. E., and Olson, J.A., 1986, Map showing faults and earthquake epicenters in San Mateo County, California: U.S. Geological Survey Map I-1257-F, scale 1:62,500.

Bruns, T.R., Cooper, A.K., Carlson, P.R., and McCulloch, D.S., 2002, Structure of the submerged San Andreas and San Gregorio, fault zones in the Gulf of the Farallones off San Francisco, California, from high-resolution seismic reflection data, *in* Parsons, T., ed., Crustal structure of the coastal and marine San Francisco Bay region: U.S. Geological Survey Professional Paper 1658, p. 77-117.

Chappell, J., and Shackleton, N.J., 1986, Oxygen isotopes and sea level, Nature, v. 324, p.137-140

Clifton, E.H., Hunter, R.E., Gardner, J.V., 1988, Analysis of eustatic, tectonic, and sedimentologic influences on transgressive and regressive cycles in the upper Cenozoic Merced Formation, San Francisco, *in* Kleinspehn, K.L. and Paola, C. eds, New perspectives in basin analysis: Springer-Verlag, N.Y., p.109-128.

Clifton, H.E., Hunter, R.E., 1987, The Merced Formation and related beds: A mile-thick succession of late Cenozoic coastal and shelf deposits in the sea cliffs of San Francisco, California, *in* Hill, M.L., ed., Cordilleran Section of the Geological Society of America, Centennial Field Guide, v.1, p. 257-262.

Compton, R.R., 1985, Geology in the Field: John Wiley and Sons, 398 p.

Graham, S.A., 1978, Role of Salinian Block in evolution of San Andreas fault system, California: AAPG Bulletin, v. 62, p. 2214-2231.

Hall, N.T., 1965, Petrology of the type Merced Group, San Francisco Peninsula, California [M.A. thesis]: University of California, Berkeley, 127 p.

Hunter, R.E., and Clifton, H.E., 1982, Description of beds exposed at Fort Funston, Golden Gate National Recreation Area, Northwestern San Francisco, California: U.S. Geological Survey Open-File Report 82-1055, 30 p.

Hunter, R.E., Clifton, H.E., Hall, N.T., Crasser, G., Richmond, B.M., and Chin, J.L., 1984, Pliocene and Pleistocene coastal and shelf deposits of the Merced Formation and associated beds, northwestern San Francisco Peninsula, California: Society of Economic Paleontologist and Mineralogists Field Trip Guidebook, v. 3, p. 1-30.

Ingram, B.L., and Ingle, J.C., 1998, Strontium isotope ages of the Marine Merced Formation, near San Francisco, California: Quaternary Research, v. 50, p. 194-199.

Jachens, R.C., and Zoback, M.L., 1999, The San Andreas fault in the San Francisco Bay region, California, Structure and kinematics of a young plate boundary, *in* Ernst, W. G. and Coleman, R.G., eds., Tectonic Studies of Asia and the Pacific Rim: Geologic Society of America, International Book Series, v. 3, p. 217-231.

Jennings, C.W., Strand, R.G., Rogers, T.H., 1977, Geologic Map of California: California Division of Mines and Geology, scale 1:750,000.

Jennings, C.W., Saucedo, G.J., Toppozada, T., Branum, D., 2002, Simplified fault activity map of California: California Geological Survey, scale 1:2,500,000.

Kennedy, D.G., 2002, Neotectonic character of the Serra Fault, northern San Francisco Peninsula, California [M.S. thesis]: San Francisco State University, 117 p.

Lajoie, K. R. 1996, Northeast Santa Cruz Mountains thrust/fold belt, *in* Jayko, A.S., and Lewis, S.D, eds., Toward assessing the seismic risk associated with blind faults, San Francisco Bay Region, California: U.S. Geological Survey Open-File Report 96-267, p. 86-104.

Lanphere, M. A., Champion, D.E., Clynne, M.A., Lowenstern, J.B., Sarna-Wojcicki, A.M., Wooden, J.L., 2004, Age of the Rockland tephra, western USA: Quaternary Research, v. 62, p. 94-104.

Lisiecki, L.E., and Raymo, M.E., 2005, A Pliocene-Pleistocene stack of 57globally disturbed benthic delta (super 18) O records: Paleoceanography, v. 20, 17 p.

Luhdorff & Scalmanini Consulting Engineers, Inc. (LSCE), 2004, Update in the conceptualization of the lake aquifer system, Westside groundwater basin, San Francisco and San Mateo Counties.

Luhdorff & Scalmanini Consulting Engineers, Inc. (LSCE), 2006, Hydrogeologic conditions in the Westside Basin.

Matthews, V., 1976, Correlation of Pinnacles and Neenach volcanic formations and their bearing on San Andreas fault problems: AAPG Bulletin, v. 60, p. 2128-2141.

McLaughlin, R.J., Langeheim, V.E., Schmidt, K.M., Jachens, R.C., Stanley, R.G., Jayko, A.S., McDougall, K.A., Tinsley, J.C., and Valin, Z.C., 1999, Neogene contraction between the San Andreas fault and the Santa Clara Valley, San Francisco Bay Region, California: International Geology Review, v. 41, p. 1-30.

Meyer, C.E., Sarna-Wojcicki, A.M., Hillhouse, J.W., Woodward, M.J., Slate, J.L., and Sorg, D.H., 1991, Fission track age (400,000 yr) of the Rockland Tephra, based on inclusion of zircon grains lacking fossil fission tracks: Quaternary Research, v. 35, p. 367-382.

Nzewi, O., 2007, 2006 Annual groundwater monitoring report, Westside Basin, San Francisco and San Mateo Counties, California: unpublished San Francisco Public Utilities Commission report, prepared for the City of San Francisco, 32 p.

Pampeyan, E.H., 1994, Geologic Map of the Montara and San Mateo 7.5' Quadrangles, San Mateo County California: U.S. Geological Survey Map I-2390, scale 1:24,000.

Phillips, S.P., Hamlin, S.N., and Yates, E.B., 1993, Geohydrology, water quality, and estimation of ground-water recharge in San Francisco, California, 1987-1992: U.S. Geological Survey Water-Resources Investigations Report 93-4019, 69 p.

Ring, U., 2008, Deformation and exhumatrion at convergent margins: the Francisco subduction complex: Geological Society of America Special Paper 445, 61 p.

Rogge, E.H., 2003, Dimensions of the Westside Groundwater Basin, San Francisco and San Mateo Counties, California [M.S. thesis] San Francisco State University, 200 p.

Ryan, H.F., Parsons, T., and Sliter, R.W., 2008, Vertical tectonic deformation associated with the San Andreas fault zone offshore of San Francisco, California: Tectonophysics, v. 457, p. 209-223.

Sarna-Wojcicki, A.M, Meyer, C.E., Bowman, H.R., Hall, T., Russell, P.C., Woodward, M.J., Slate, J.L., 1985, Correlation of the Rockland ash bed, a 400,000-year old stratigraphic marker in Northern California and western Nevada, and implications for middle Pleistocene paleogeography of Central California: Quaternary Research, v. 23, p.236-257.

Schlocker, J., 1974, Geology of the San Francisco North Quadrangle, California; U.S. Geological Survey Professional Paper, 782 p.

Sylvester, A.G., 1988, Strike-slip faults: Geological Society of America Bulletin, v. 100, p. 1666–1703.

Wakabayashi, J., Hengesh, J.V., Sawyer, T.L., 2004, Four-dimensional transform fault processes: progressive evolution of step-overs and bends: Tectonophysics, v. 392, p. 279-301.

Wood, K., 2008, Hydrogeologic characterization of the Northern Westside Basin, San Franicisco, California [M.S. thesis]: San Francisco State University, 102 p.

Yancey, T.E., 1978, Stratigraphy of the Plio-Pleistocene strata in the Twelvemile Creek area, San Francisco, California: Proceedings of the California Academy of Sciences, Fourth Series, v. XLI, p. 357-370.

Yi, C., 2005, Depositional and deformational history of the uppermost Merced and Colma formations, southwest San Francisco [M.S. thesis]: San Francisco State University, 137 p.

Zoback, M.L., Jachens, R.C., and Olson, J.A., 1999, Abrupt along-strike change in tectonic style: San Andreas fault zone, San Francisco Peninsula: Journal of Geophysical Research, v. 104, p. 10,719-10,742.